

Lixin Cheng *Editor*

# Frontiers and Progress in Multiphase Flow I

## Contents

<b>1 Selected Aspects of Thermal-Hydraulics Modelling in Two-Phase Flows with Phase Change in Minichannels. . . . .</b>	<b>1</b>
Dariusz Mikielewicz	
<b>2 Flow Characteristics and Void Fraction Prediction in Large Diameter Pipes. . . . .</b>	<b>55</b>
Xiuzhong Shen, Joshua P. Schlegel, Shaowen Chen, Somboon Rassame, Matthew J. Griffiths, Takashi Hibiki and Mamoru Ishii	
<b>3 Physical Water Treatment Using Oscillating Electric Fields to Mitigate Scaling in Heat Exchangers. . . . .</b>	<b>105</b>
Leonard D. Tijjing, Cheol Sang Kim, Dong Hwan Lee and Young I. Cho	
<b>4 Flow Patterns, Void Fraction and Pressure Drop in Gas-Liquid Two Phase Flow at Different Pipe Orientations . . . . .</b>	<b>157</b>
Afshin J. Ghajar and Swanand M. Bhagwat	

# Chapter 4

## Flow Patterns, Void Fraction and Pressure Drop in Gas-Liquid Two Phase Flow at Different Pipe Orientations

Afshin J. Ghajar and Swanand M. Bhagwat

**Abstract** This chapter presents an insightful discussion on flow patterns, void fraction and phenomenon of two phase frictional pressure drop in gas-liquid two phase flow. The flow structure of different flow patterns observed in gas-liquid two phase flow at various pipe orientations are described with the aid of flow visualization. This chapter is helpful in understanding the impact of varying flow patterns, pipe diameter and pipe orientation on the void fraction and two phase pressure drop. Additionally, a brief overview of the void fraction, its dependency on the flow patterns and its influence on the hydrostatic pressure drop is presented. A brief synopsis of the two phase void fraction and frictional pressure drop correlations available in the literature is presented. The performance of these correlations is assessed against a comprehensive database for air-water and refrigerant two phase flow conditions. Based on this detailed analysis, the top performing void fraction and pressure drop correlations are identified and recommended for use for these fluid combinations in different two phase flow situations. Finally, application of the recommended correlations is presented in the form of solved problems. It is expected that these solved problems will give readers an idea of selection and implementation of appropriate correlations for different two phase flow conditions.

**Keywords** Flow patterns · Void fraction · Drift flux model · Hydrostatic pressure drop · Frictional pressure drop · Gas-liquid two phase flow · Two phase frictional multiplier · Two phase dynamic viscosity

### Nomenclature

$B_{Ch}$  Variable in (Chisholm [20]) correlation  
 $C_o$  Distribution parameter  
 $D$  Pipe diameter (m)  
 $f$  Friction factor

---

A. J. Ghajar (✉) · S. M. Bhagwat  
School of Mechanical and Aerospace Engineering, Oklahoma State University,  
Stillwater, OK 74078, USA  
e-mail: afshin.ghajar@okstate.edu

Fr	Froude number ( $Fr = G^2/(gD\rho^2)$ )
g	Acceleration due to gravity (9.81 m/s <sup>2</sup> )
G	Mass flux (kg/m <sup>2</sup> s)
Ku	Kutateladze number as defined by Takeuchi et al. [97]
L	Pipe length (m)
La	Laplace number ( $La = \sqrt{\sigma/g(\rho_l - \rho_g)}/D$ )
$N_{\mu f}$	Viscosity number ( $N_{\mu f} = \mu_l / (\rho_l \sigma \sqrt{\sigma/g\Delta\rho})^{0.5}$ )
P	Pressure (Pa)
Re	Reynolds number ( $Re = (GD)/\mu$ )
S	Slip ratio
U	Phase velocity (m/s)
$U_{gm}$	Drift velocity (m/s)
We	Weber number ( $We = (G^2D)/(\sigma\rho)$ )
x	Two phase quality
X	(Lockhart and Martinelli [66]) parameter

### Greek Symbols

$\alpha$	Void fraction
$\beta$	Gas volumetric flow fraction
$\rho$	Phase density (kg/m <sup>3</sup> )
$\mu$	Phase dynamic viscosity (Pa-s)
$\theta$	Pipe orientation (degrees)
$\sigma$	Surface tension (N/m)
$\Phi^2$	Two phase frictional multiplier

### Subscripts

a	Accelerational
atm	Atmospheric
crit	Critical
f	Frictional
g	Gas
go	Gas only
h	Hydrostatic
in	Inlet
j	Phase
l	Liquid
lo	Liquid only
m	Mixture
out	Outlet
s	Superficial
sys	System
t	Total

tp	Two phase
tt	Turbulent-turbulent
w	Water

**Superscript**

\* Non-dimensional parameter

## 4.1 Introduction

Gas-liquid two phase flow finds its extensive application in the industrial processes pertaining to oil-gas, chemical, nuclear and refrigeration industries. The two component two phase flow referred to as non-boiling flow or two phase flow without undergoing phase change is often encountered in industrial applications such as artificial lift systems and simultaneous transportation of oil and natural gas from remote extraction locations to the processing units. Chemical operations requiring flow of two chemical species together for enhanced mass transfer as in case of ozone treatment of water also relies on gas-liquid non-boiling two phase flow phenomenon. One component two phase flow i.e., the boiling/condensation flow or two phase flow undergoing a phase change process is always present in the nuclear safety operations required for cooling of nuclear reactor rods and in heat exchangers where refrigerants undergo phase change process in evaporators and condensers. For refrigerant two phase flow, the correct estimation of void fraction is required to determine the refrigerant charge inventory while the correct estimation of pressure drop is desired as it influences the refrigerant saturation temperature and hence the overall system efficiency. Irrespective of the type of flow i.e., boiling and non-boiling, for a design engineer the proper understanding of two phase flow phenomenon is of utmost importance for designing of these operations and sizing of process equipment.

For any industrial process from design point of view, the total pressure drop that occurs in the system is of concern which in turn depends strongly on correct understanding of the flow patterns and accurate prediction of the void fraction. The first step in prediction of total pressure drop is the estimation of hydrostatic two phase pressure drop that requires understanding of the flow pattern and accurate estimation of the void fraction at any given pipe orientation, pipe diameter and flow rates of individual phases. The knowledge of flow patterns is necessary since the frictional pressure drop in two phase flow is sensitive to the distribution of gas and liquid phase across the pipe cross section and along the pipe length. Both the flow patterns and void fraction are observed to change with change in flow patterns and pipe orientation and thus result in significantly different pressure drop even measured at similar phase mass flow rates but at different pipe orientations. In order to address these issues with better understandings, one of the objectives of

this work is to discuss the effect of different two phase flow variables on the flow patterns, void fraction and hence the pressure drop in two phase flow.

So far an extensive research has been carried out in the general area of two phase flow that has contributed in improving overall understanding of two phase flow phenomenon, development of theories and models to predict flow patterns, void fraction and pressure drop. However, all these developments are confined to certain two phase flow scenarios in terms of pipe geometry and orientations, fluid physical properties and flow patterns and hence fail to predict the desired outcome correctly if arbitrarily used against different two phase flow conditions. Moreover, the majority of this research is focused on the gas-liquid two phase flow in horizontal and vertical upward pipe orientation while comparatively rare information is available on the behavior of two phase flow in upward and downward inclined pipes. The challenging part of solving a two phase flow problem is correct identification of the flow pattern for given set of flow conditions since, the flow patterns are defined on a qualitative basis without any physical parameter to quantify the occurrence of a particular flow pattern at given phase flow rates, pipe geometry and fluid physical properties. The definition of flow pattern depends upon an individual's perception and hence involves the risk of using a wrong correlation to predict the void fraction and pressure drop due to incorrect recognition of the flow pattern.

Thus it is strongly desired to have correlations that can predict void fraction and two phase frictional pressure drop independent of the flow pattern, pipe orientation and pipe diameter. To explore and discuss this issue, the scope of this chapter includes the performance assessment of different correlations that can predict void fraction and two phase frictional pressure drop independent of the flow patterns. The performance of these correlations is assessed against a comprehensive data bank for two phase void fraction and pressure drop in different pipe diameters and pipe orientations available with Two Phase Flow Lab, Oklahoma State University. Based on this assessment, the top three performing correlations are identified for various two phase flow conditions and are recommended to use in prediction of void fraction and two phase frictional pressure drop.

## **4.2 Flow Patterns and Flow Patterns Map**

The flow patterns in gas-liquid two phase flow are generated due to significantly different physical properties of gas and liquid phase, compressibility nature of the gas phase and their alignment with respect to each other across the pipe cross section. The knowledge of flow patterns and flow pattern maps proves instrumental in the general understanding of the physical structure and the mechanism of momentum and heat transfer in two phase flow. The flow pattern map serves as a tool to estimate the sequence of the appearance of different flow patterns with change in the gas and liquid flow rates for a given set of flow conditions. The definitions of flow patterns and their transitions are highly qualitative in nature and

are mostly based on the individual's perception. Although some researchers have attempted to develop quantitative methods such as the probabilistic flow regime mapping to predict the existence of certain flow patterns these methods are not universal and are mostly limited to certain flow conditions. The purpose of this section is to present an overview of the flow patterns and the similarities and differences in the physical structure of flow patterns observed in horizontal, vertical upward and vertical downward pipe orientations. The flow pattern maps presented in this section are exclusively developed for two phase flow of air water through a 12.5 mm I.D. pipe at different orientations and are not generic. The objective of introducing these flow patterns maps is to give readers an idea about the effect of pipe orientation on the transition between different flow patterns for fixed pipe diameter and fluid combination.

Let's first look at the physical structure of two phase flow patterns at different pipe orientations. The vertical upward and downward flow share some flow patterns such as bubbly, slug, froth and annular flow in common while the churn flow is observed in vertical upward flow and falling film is observed only in vertical downward orientation. The horizontal flow direction allows existence of bubbly, slug, stratified, wavy and annular flow patterns. Bhagwat and Ghajar [13] illustrated that the two extreme opposite flow directions namely, vertical up and vertical down pipe orientations significantly influence the general appearance of the flow patterns and their transition from one to another. The flow visualization of the bubbly and slug flow show a significant influence of the flow direction on the alignment of one phase with respect to another. These differences in the physical structure of the flow patterns are essentially due to the interaction between buoyancy, gravity and inertia forces. As shown in Fig. 4.1, in case of the vertical upward bubbly flow, the bubbles are distributed evenly across the pipe cross section in the continuous liquid medium for almost all combinations of liquid and gas flow rates. Whereas, the bubbles in vertical downward flow tend to flow in a region close to the pipe center due to repulsion exerted from the pipe wall (known as coring phenomenon) as a function of interaction between buoyancy and inertia forces. With increase in the liquid and gas flow rates, the inertia forces supersede the buoyancy effects and hence the wall repulsion force. Consequently, bubbles start to move towards pipe wall and get more evenly distributed throughout the pipe cross section and finally the physical appearance of the bubbly flow is similar in both vertical upward and downward flow directions. Nguyen [76], Oshinowo [80] and Usui and Sato [102] reported similar type of observations for the coring phenomenon in 19, 25 and 45 mm I.D. vertical downward pipes. It should be noted that the coring phenomenon occurs only in vertical downward pipe orientation and is prominent for large diameter pipes. It is anticipated that the coring phenomenon vanishes with decrease in the pipe diameter since two phase flow literature doesn't provide any evidence of its existence for pipe diameters typically  $D < 12$  mm. This difference in general appearance of the bubbly flow is observed to have noticeable effect on the two phase frictional pressure drop in vertical upward and downward flows. In case of the horizontal two phase flow, the bubbles are always observed to flow in the vicinity of the pipe upper wall due to the buoyancy effects

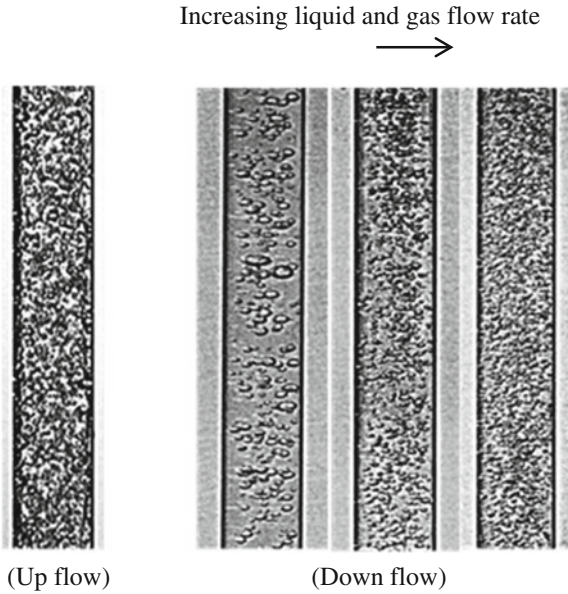


**Fig. 4.1** Physical appearance of bubbly flow in vertical upward and downward pipe orientation

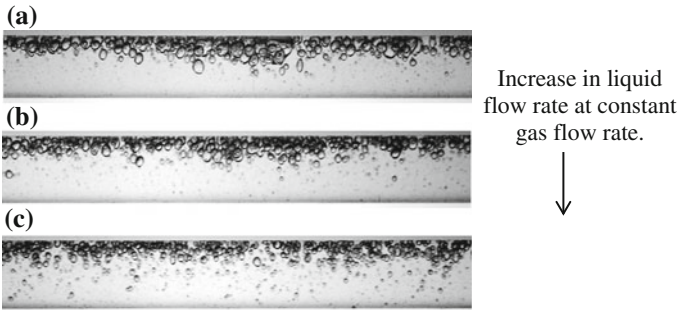
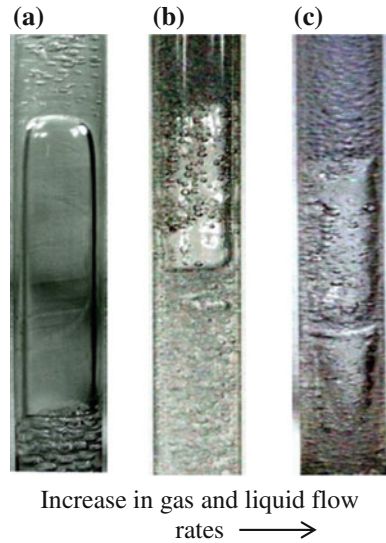


**Fig. 4.2** Two phase bubbly flow in horizontal pipe orientation

as shown in Fig. 4.2. At fixed gas flow rate, increase in the liquid flow rate results in the shearing of gas bubbles that reduces its size (Figs. 4.2a, b), and consequently increase the number of bubbles that try to penetrate the single phase liquid and enter the near pipe axis region (Fig. 4.2c).

The slug flow regime in vertical upward, downward and horizontal pipe orientations resembles in general appearance i.e., the slug flow in all of these three orientations is characterized by the alternate flow of liquid and elongated gas bubbles. However, a close observation reveals some differences in the shape of the nose and tail region of the slug in addition to the effect of pipe orientation on slug flow direction. The slug in vertical upward orientation appears as a bullet shaped elongated gas bubble pointing in upward direction (due to buoyancy acting in flow

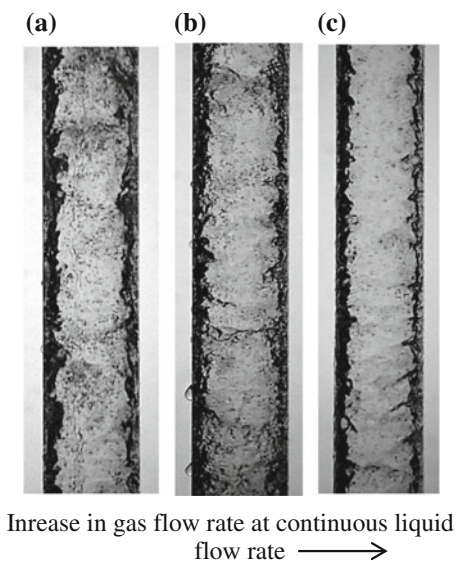
**Fig. 4.3** Slug flow in vertical downward two phase flow



direction) while the slug in vertical downward flow can have three possible shapes. Bhagwat and Ghajar [13] have identified that the slug flow in vertical downward orientation initially shows a blunt bubble nose pointing in upward direction for the low values of gas and liquid flow rates. As shown in Fig. 4.3, with increase in both gas and liquid flow rates, the bubble nose becomes flat (Figs. 4.3a, b) and finally appears pointing downwards in the direction of net flow with further increase in the flow rates (Fig. 4.3c). These three different shapes of the slug are essentially due to the balance between the buoyancy and inertia forces. The shape of these slugs also affects their translational velocity through the pipe. Based on the visual observations it is seen that the velocity of downward pointing slug is relatively greater than the velocity of a upward pointing blunt nose shaped slug and flat headed slug. Literature reports that these different forms of vertical downward slug flow exist only for a certain range of pipe diameter approximately for  $10 \text{ mm} < D < 50 \text{ mm}$ . It should be noted that the different motions and shapes of gas slug may affect the two phase pressure drop and heat transfer characteristics and hence it is very important to understand the transition (in terms of the phase velocity known as bubble turning velocity) between these different forms of slug flows. However, literature lacks reliable methods to provide information on this transition as a function of fluid combination and pipe diameter.

The froth and churn flow regimes in vertical upward flow has no definitive physical structure and hence their flow visualization is not reported here. The falling film flow in vertical downward flow occurs at low liquid and moderate gas flow rates and is characterized by the flow of liquid gliding smoothly over the pipe surface while the gas phase flows through the core. This type of flow is mostly encountered in film type vertical downward condensers. A major precaution that needs to be taken while operating in the non-isothermal falling film flow regime is

**Fig. 4.4** Two phase annular flow in vertical upward pipe orientation



to avoid dry spots on the pipe wall due to excess amount of heat transfer that may further lead to system damage. Since there is no major difference in the physical structure of the falling film flow even with increase in the gas and liquid flow rates, its flow visualization is not reported. The annular flow regime in both vertical upward and downward pipe orientations can be described as the flow of turbulent gas core inside a wavy liquid annulus in contact with the pipe wall. In case of vertical upward and downward flow, there is symmetry about the pipe axis and hence the film thickness can be assumed to be the same throughout the pipe circumference. Whereas, in case of horizontal flow, the flow nature is asymmetric about the pipe axis and the liquid film thickness near the pipe bottom wall is greater than the pipe upper wall due to gravity acting on liquid phase. The gas-liquid interface is wavy and continuous but is dynamic in nature. The liquid film thickness is found to be a function of flow rates, pipe diameter, and orientation and fluid properties. As shown in Figs. 4.4(a–c) and 4.5(a–c), for a fixed pipe diameter ( $D = 12.5$  mm) and fluid combination (air-water), the liquid film thickness is observed to decrease with increase in the gas flow rate due to the shearing action of gas phase on continuous liquid phase. The annular two phase flow is studied extensively in the literature due to enhanced pressure drop and heat transfer characteristics in this flow regime.

The sequence and the transition of above discussed key flow patterns in horizontal, vertical upward and downward pipe orientations are presented in terms of flow pattern maps in Figs. 4.6, 4.7 and 4.8, respectively. In case of horizontal flow, bubbly flow appears for high liquid and low gas flow rates. Plug flow appears at relatively moderate liquid and low gas flow rates and with increase in the gas flow rate, the flow pattern shifts to slug, wavy slug and finally to annular flow regime. Similar sequence of flow patterns appearance is found in case of vertical upward

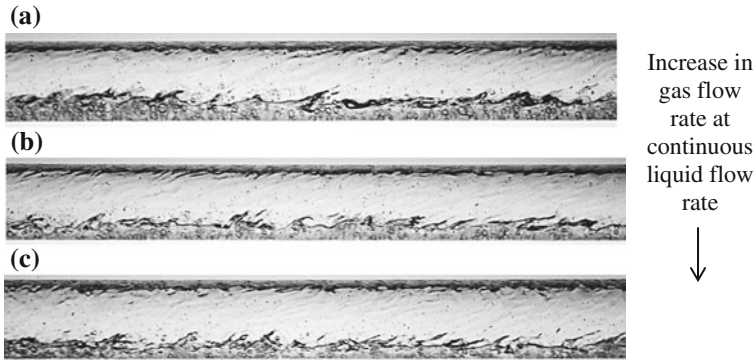


Fig. 4.5 Two phase annular flow in horizontal pipe orientation

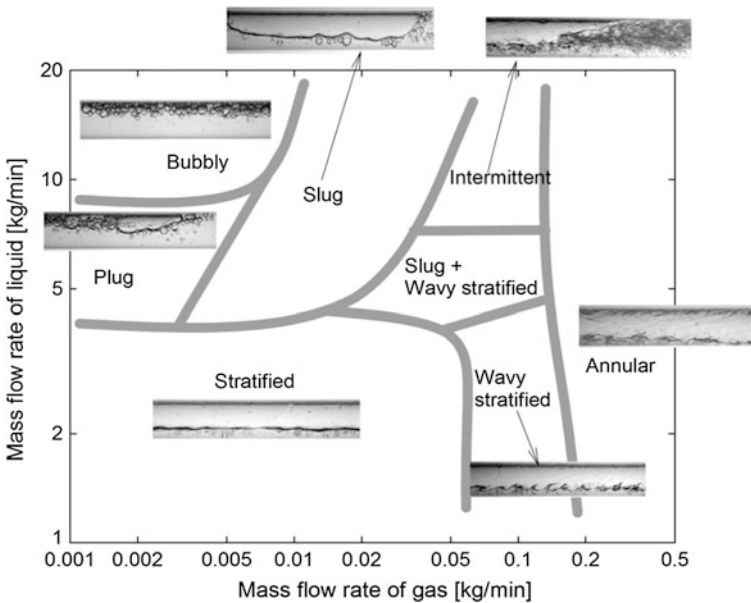


Fig. 4.6 Flow pattern map for horizontal flow

and downward pipe orientations. However, a noticeable difference in the transition boundaries is observed among these three orientations. In comparison to vertical upward and downward flow, the horizontal bubbly flow occupies a small region on the flow pattern map. It appears at comparatively high liquid mass flow rates and transits to slug flow quickly at the maximum gas mass flow rate of 0.1 kg/min. In case of vertical upward orientation, the slug flow exists at smaller liquid and gas flow rates compared to vertical downward and horizontal pipe orientations. This is probably due to the fact that, the net upward flow assists the buoyancy of the gas slug and thus this flow pattern requires smaller gas flow rates to appear.

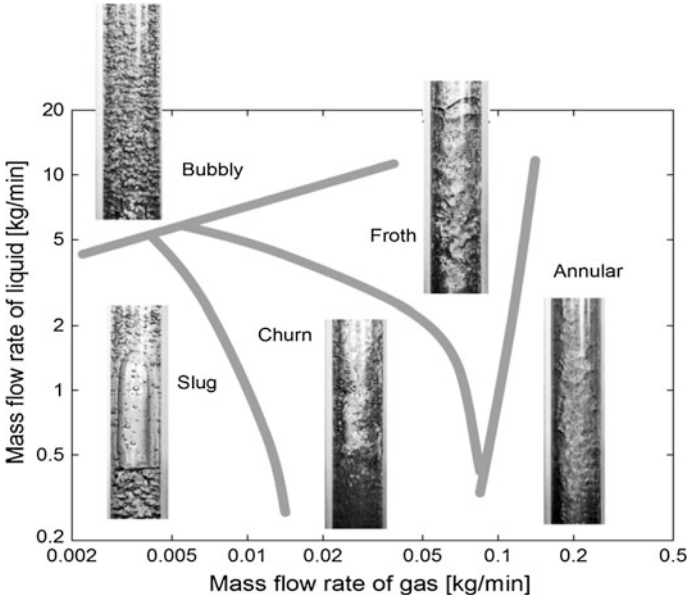


Fig. 4.7 Flow pattern map for vertical upward flow

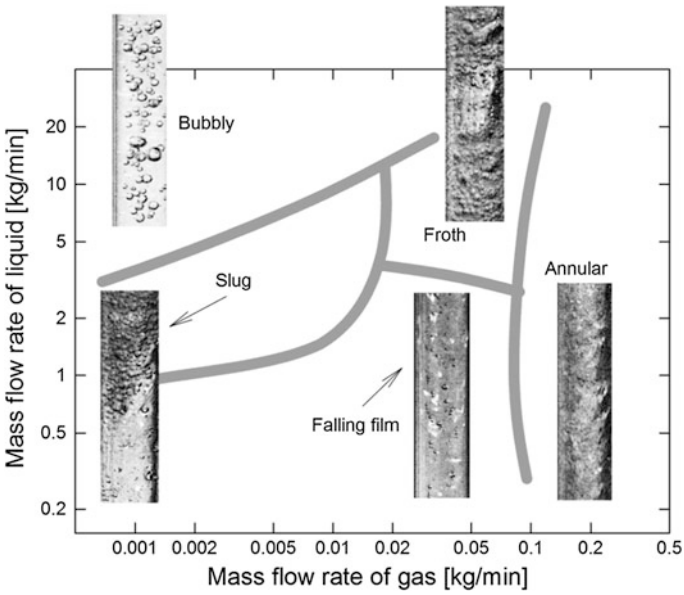


Fig. 4.8 Flow pattern map for vertical downward flow

Although some divergence is observed for the churn annular transition line at low liquid mass flow rates in vertical upward flow; the transition line that separates the annular flow pattern from other flow patterns has approximately the same trend for vertical upward, downward and horizontal pipe orientations. Stratified flow exists for horizontal, downward inclined and near horizontal upward inclined pipe orientations. Experimental flow visualization work of [42] has shown that the transition line in horizontal flow pattern map that separates stratified flow from other flow patterns go away with increase in upward inclined pipe orientations while there is a little effect on transition between other flow patterns with change in pipe orientation from  $0^\circ$  to  $+7^\circ$  from horizontal.

It should be noted that the flow pattern maps reported here are specific to the experimental setup at Two Phase Flow Lab, Oklahoma State University and the transition boundaries between different flow patterns may alter with change in fluid properties, pipe diameter and pipe orientation. Also as mentioned earlier, since there is no reliable quantitative tool available in the literature to predict the existence and transition of one flow pattern to another for varying two phase flow conditions it is always recommended to use the void fraction and pressure drop correlations that are independent of the flow pattern but still account for the relevant two phase flow physics.

### **4.3 Void Fraction in Gas-Liquid Two Phase Pipe Flow**

As mentioned earlier, the void fraction in gas liquid two phase flow is an indispensable parameter required in several calculations such as the estimation of two phase mixture density required in calculation of two phase hydrostatic pressure drop and the refrigerant charge inventory. The knowledge of void fraction is also crucial in thermo-hydraulic simulations and in determination of two phase natural circulation loop flow rates and the corresponding heat transfer rates. Void fraction in gas-liquid two phase flow is found to be a function of several parameters such as the flow patterns, fluid properties and pipe diameter and orientation. In comparison to the effect of fluid properties and pipe diameter, the effect of flow patterns and pipe orientation on the void fraction is more prominent. The purpose of this section is to report the relationship between void fraction, flow patterns and pipe orientation.

#### ***4.3.1 Effect of Flow Patterns (Phase Flow Rates) on Void Fraction***

The void fraction in gas-liquid two phase flow is sensitive to the flow patterns. Irrespective of the pipe diameter, orientation and fluid properties, the void fraction increases sharply with a small increase in the gas flow rate for bubbly and slug flow regimes. Whereas, in case of the annular flow, the void fraction is observed to

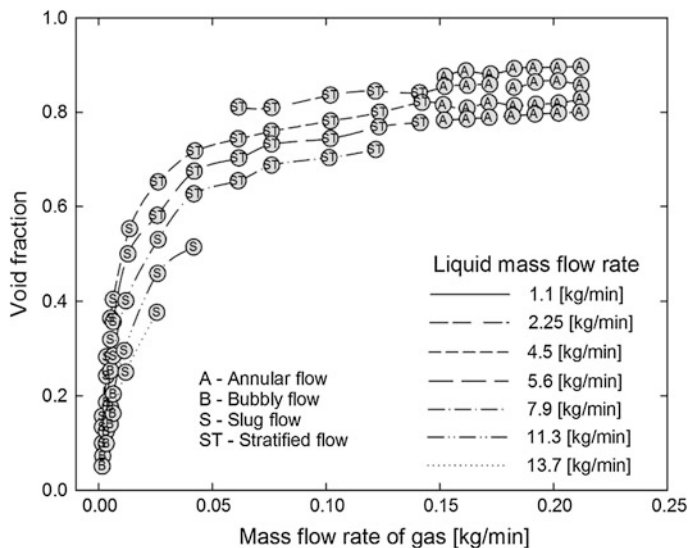


**Fig. 4.9** Variation of void fraction with change in the gas and liquid flow rates for different flow patterns in horizontal flow

remain nearly constant even with a major increase in the gas flow rate. The general trend of the increase in void fraction with increase in gas flow rate for various flow patterns in non-boiling horizontal, vertical upward and vertical downward two phase flow is shown in Figs. 4.9, 4.10 and 4.11, respectively. The experimental data is collected for air-water fluid combination in a 12.5 mm I.D. polycarbonate pipe at Two Phase Flow Lab, Oklahoma State University.

### 4.3.2 Effect of Pipe Orientation on Void Fraction

Regardless of whether or not the flow is boiling or non-boiling in nature, the void fraction in gas-liquid two phase flow is observed to be a strong function of the pipe orientation. In comparison to horizontal and vertical pipe orientations the experimental work related to void fraction and pressure drop in upward and downward inclined pipe orientations is limited. Some of the experimental work available in the literature for inclined two phase flow conditions are those of [10, 74, 76] for non-boiling flow and that of [65] for boiling two phase flow. All of these studies report a noticeable effect of the pipe orientation on void fraction. As shown in Fig. 4.12, for fixed flow conditions, the void fraction first decreases and then increases with increase in the pipe inclination in upward direction. In case of downward inclinations measured from horizontal, the void fraction first increases and later decreases with increase in the pipe orientation. The void fraction is maximum for vertical downward flow in comparison to horizontal and vertical

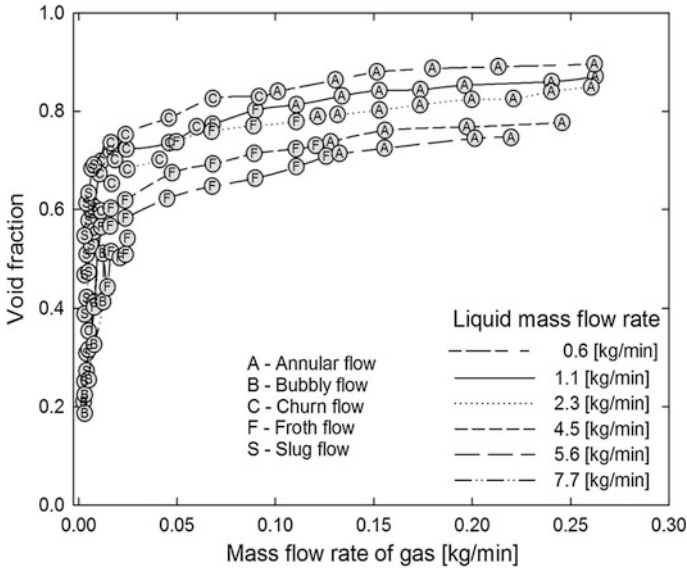


**Fig. 4.10** Variation of void fraction with change in the gas and liquid flow rates in vertical upward flow

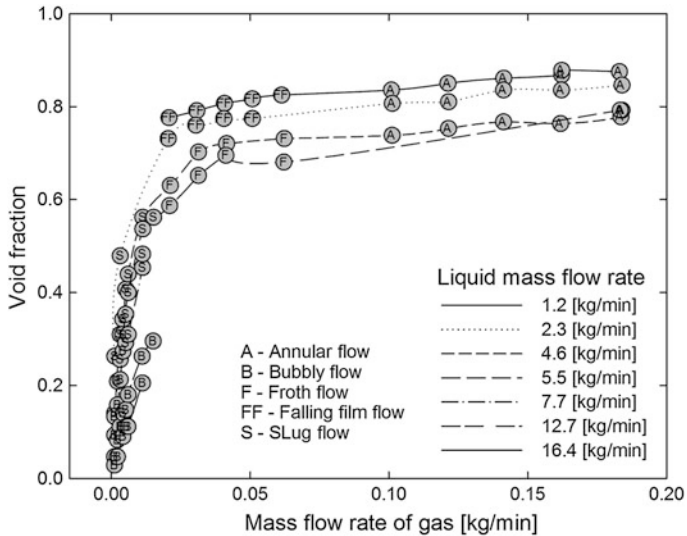


**Fig. 4.11** Variation of void fraction with change in the gas and liquid flow rates in vertical downward flow

upward flow. In case of boiling two phase flow, the minima in void fraction is observed to shift towards lower inclination from horizontal with increase in the two phase mixture quality. Another interesting trend observed for boiling two

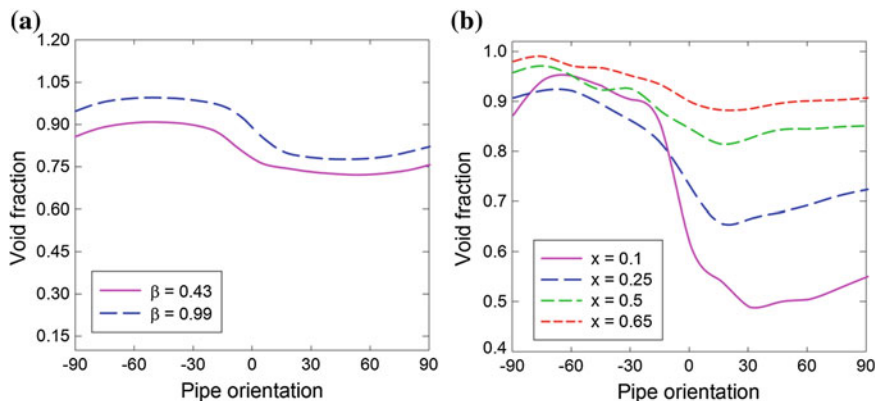


**Fig. 4.12** Effect of pipe orientation on void fraction. **a** Non boiling flow (air-water) data from [10]. **b** Condensing flow (R134a) data from [65]

phase flow is that, with increase in the two phase quality, the effect of pipe orientation on void fraction diminishes and thus it is expected that for very high qualities, void fraction remain virtually unaffected by the pipe orientation.

This effect of the pipe orientation on the void fraction can be explained with the help of the concept of residence time of the gas phase inside a given pipe section. For instance, when the void fraction is measured using quick closing valves (QCV) then, the amount of gas phase trapped in the given pipe section depends upon the relative magnitudes of buoyancy, inertia and gravity forces. In case of vertical downward flow, the buoyancy and inertia forces are opposite in direction that opposes the mean flow and hence results into higher residence time of the gas phase and hence higher void fraction. In contrast to this, the residence time of the gas phase in the upward flow is lower where the buoyancy complements the mean direction of two phase flow and hence results in lower values of void fraction. Above discussion infers that the void fraction in downward inclined flow is higher than that in upward inclined two phase flow. From Fig. 4.12, it can also be concluded that the relative magnitude of buoyancy and inertia forces change at certain inclinations from horizontal and that causes shift in the trend of void fraction at these pipe orientations. Since, the effect of buoyancy forces will go away with decrease in the pipe diameter, it can be anticipated that the effect of pipe orientation at fixed flow conditions is more prominent for large pipe diameters and is negligible for very small pipe diameters.

### 4.3.3 Effect of Pipe Diameter on Void Fraction

The effect of pipe diameter on gas-liquid void fraction is not as significant as the flow patterns or the pipe orientation. The effect of pipe diameter on void fraction for flow of R410A in horizontal pipe orientation is shown in Fig. 4.13. It is evident

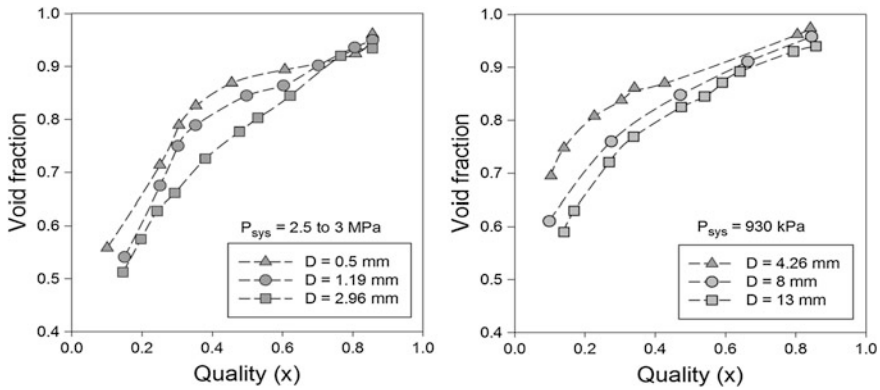


**Fig. 4.13** Effect of pipe diameter on void fraction in horizontal two phase flow of R410A

that the void fraction increases with decrease in the pipe diameter for low values of quality or typically in bubbly and slug flow regimes. The effect of pipe diameter is observed to vanish gradually with increase in the two phase flow quality. This observation is in agreement with the work of [55] who investigated the effect of pipe diameter in a range of  $5 \text{ mm} < D < 50 \text{ mm}$  on void fraction in vertical upward annular flow regime for non-boiling two phase flow. They found that the effect of pipe diameter on void fraction in the annular flow regime is negligible. Due to lack of experimental data for similar fluid combinations the effect of pipe diameter on two phase pressure drop for various pipe orientations could not be analyzed. However, based on the trend of the data in Fig. 4.13 for horizontal two phase flow and the results of [55] for vertical upward flow, it can be conjectured that the effect of pipe diameter on void fraction is independent of the pipe orientation for annular flow regimes. More experimental data and in-depth analysis is required to verify this effect for other flow patterns.

From the discussion so far, it is evident that void fraction is influenced by the flow patterns, pipe orientation and pipe diameter. Thus, for successful prediction of the void fraction it is very much desired for any correlation to account for the effect of pipe orientation, pipe diameter and flow patterns on the void fraction.

#### 4.4 Performance Assessment of Two Phase Void Fraction Correlations

Since last few decades, significant contribution has been made by the scientific community to experimental measurements and modeling of void fraction in gas-liquid two phase flow. The initial experimental and modeling work in this field was mostly focused on the air-water two phase flow and later got diversified by the inclusion of boiling two phase flow phenomenon encountered in refrigeration and

nuclear industry and the simultaneous flow of oil-gas commonly observed in petroleum industry. In spite of the numerous void fraction correlations available in the literature, there is no single correlation that can be relied upon to predict the void fraction correctly for a wide range of two phase flow situations. Most of these available correlations have limited application due to the restrictions imposed on them for certain fluid combinations, pipe orientations and pipe diameters. As a result, the main problem for a design engineer is to make a correct choice of the void fraction correlation for the desired application. The objective of this section is to revisit some of the renowned and widely used void fraction correlations and recommend the rigorously scrutinized top performing correlations for air-water and refrigerant two phase flow for a range of pipe diameters and pipe orientations.

The void fraction correlations reported in the literature can be broadly classified in three main categories. For instance, the correlations based on the concept of the slip (separated flow) model, the drift flux model and empirical correlations. The slip (separated flow) model based correlations assume that the two phases flow separately with different velocities and share a definite interface. The flow patterns such as stratified and annular flow behave as a separated flow and can be effectively modeled using these types of correlations. The slip model based correlations are mostly preferred in refrigeration industry due to the stratified and annular flow pattern dominated two phase flow in evaporators and condensers. The category of drift flux model based correlations assumes one phase dispersed in other continuous phase and requires the determination of distribution parameter and drift velocity as variables to calculate void fraction. The flow patterns such as bubbly flow, slug flow and mist flow are the preferred flow patterns to be modeled using the concept of drift flux. The application of empirical correlations is mostly restricted by the range of experimental data used to determine the constants and hence tend to fail if used for a wide range of flow conditions out of the scope of that particular correlation.

Let's first consider some of the widely used separated flow model based void fraction correlations reported in the literature. The general form of the separated flow model may be expressed as shown in Eq. (4.1).

$$\alpha = \frac{1}{1 + \left(\frac{1-x}{x}\right) \left(\frac{\rho_g}{\rho_l}\right) S} \quad (4.1)$$

The slip ratio ( $S$ ) in Eq. (4.1) is the ratio of actual cross sectional averaged velocities of the gas and liquid phase as expressed by Eq. (4.2).

$$S = \frac{U_g}{U_l} = \frac{(U_{sg}/\alpha)}{(U_{sl}/(1-\alpha))} \quad (4.2)$$

With the homogeneous flow model assumption of equal velocities of both gas and liquid phase, the slip ratio ( $S$ ) in above equation is equal to unity. However, in reality  $S \geq 1$  or  $S < 1$  depending upon the pipe orientation and hence the above equation is modified by different investigators to account for the slippage between gas and liquid phase. The assumption of homogeneous flow remains valid only for certain region of two phase flow where  $S \approx 1$  as in case of very small region of

**Table 4.1** Void fraction correlations based on slip (separated) flow model

Correlation	A	p	q	r
homogeneous	1	1	1	0
[114]	1	1	0.67	0
[101]	1	0.72	0.4	0.08
[66]	0.28	0.64	0.36	0.07
[98]	1	1	0.89	0.18
[7]	1	0.74	0.65	0.13
[93]	2.22	0.65	0.65	0
[19]	0.18	0.6	0.33	0.07
[113]	$\alpha^{-0.125}$	0.875	0.875	0.875
[91]	$0.4 + 0.6\sqrt{\left(\frac{\rho_l}{\rho_g} + 0.4\left(\frac{1-x}{x}\right)\right) / \left(1 + 0.4\left(\frac{1-x}{x}\right)\right)}$	1	1	0
[83]	$1 + 1.578\text{Re}_{sl}^{-0.19}\left(\frac{\rho_l}{\rho_g}\right)^{0.22}\left(\frac{y}{1+yF_2} - yF_2\right)$ $y = \left(\frac{(1-x)\rho_g}{x\rho_l}\right)^{-1}, F_2 = 0.0273\text{We}_{sl}\text{Re}_{sl}^{-0.51}\left(\frac{\rho_l}{\rho_g}\right)^{-0.08}$	1	1	0
[20]	$\sqrt{1 - x\left(\frac{\rho_l - \rho_g}{\rho_l}\right)}$	1	1	0

void fraction (bubbly flow) or very large region of void fraction (annular mist flow). The general form of separated flow models that account for the slip between the two phases may be expressed by rewriting Eq. (4.1) as shown in Eq. (4.3). The different correlations are listed in Table 4.1.

$$\alpha = \frac{1}{1 + A\left(\frac{1-x}{x}\right)^p\left(\frac{\rho_g}{\rho_l}\right)^q\left(\frac{\mu_l}{\mu_g}\right)^r} \tag{4.3}$$

The void fraction correlations based on drift flux model expressed by Eq. (4.4) require determination of distribution parameter ( $C_o$ ) and drift velocity ( $U_{gm}$ ) as listed in Table 4.2.

$$\alpha = \frac{U_{sg}}{C_o U_m + U_{gm}} \text{ (where } U_m = U_{sg} + U_{sl}) \tag{4.4}$$

The performance of the void fraction correlations based on separated flow model and drift flux model considered in Tables 4.1 and 4.2 is assessed against a comprehensive data of air water and liquid refrigerant and its vapor consisting of 5162 (27 sources) and 645 (8 sources) data points, respectively. The experimental data used for performance assessment is summarized in Tables 4.3 and 4.4. The air water data consists of horizontal, upward and downward inclined pipe orientations while the refrigerant liquid vapor data consists of horizontal pipe orientation only.

The performance of separated flow model and drift flux model based correlations is assessed based on the percentage of data points predicted within certain error bands criterion for four different ranges of the void fraction namely,  $0 < \alpha \leq 0.25$ ,  $0.25 < \alpha \leq 0.5$ ,  $0.5 < \alpha \leq 0.75$  and  $0.75 < \alpha < 1$ , respectively. These four ranges

**Table 4.2** Void fraction correlations based on drift flux model

Correlation	Distribution parameter	Drift velocity (m/s)
[12]	$C_o = \left[ \frac{1}{(1+\cos\theta)^{0.25}} \right]^{(1-x)^{0.5}} + 0.18 \left( \frac{U_{sg}}{U_m} \right)^{0.1}$	$U_{gm} = (\mu_l/\mu_w)^{-0.25} (0.35 \sin\theta + 0.54 \cos\theta) \sqrt{gD(\Delta\rho/\rho_l)} (1-\alpha)^{-0.5 \sin\theta}$
[105]	$C_o = \frac{U_{sg}}{U_m} \left( 1 + \left( \frac{U_{sg}}{U_m} \right)^{b_1} \right)$ where $b_1 = \left( \frac{\rho_x}{\rho_l} \right)^{0.1}$	$U_{gm} = 2.9 [gD\sigma(1 + \cos\theta)\Delta\rho/\rho_l^2]^{0.25} (1.22 + 1.22 \sin\theta)^{b_2}$ where $b_2 = (P_{ann}/P_{sys})$ The leading constant of 2.9 carries units of $m^{-0.25}$
[86]	$C_o = 1 + 0.2(1-x)(gD\rho_l^2/G^2)^{0.25}$	$U_{gm} = 1.18(1-x)(\sigma g\Delta\rho/\rho_l^2)^{0.25}$
[45]	$C_o = 1 + 0.12(1-x)$ (for horizontal flow)	$U_{gm} = 1.53(g\sigma\Delta\rho/\rho_l^2)^{0.25} (1-\alpha)^{0.5} \sin\theta$
[15]	$C_o = 1.2$	$U_{gm} = 0.35 \sqrt{gD(\Delta\rho/\rho_l)}$
[47]	$C_o = 1$	$U_{gm} = 0.671 \sqrt{gD}(\sin\theta)^{0.263}$
[52] <sup>a</sup>	For $0 \leq (U_{sg}^+/U_m^+) \leq 0.9$ where $U_{sg}^+ = U_{sg} / (\sigma g\Delta\rho/\rho_l^2)^{0.25}$ , $U_m^+ = U_m / (\sigma g\Delta\rho/\rho_l^2)^{0.25}$ $C_o = \exp \left\{ 0.475 \left( \frac{U_{sg}}{U_m} \right)^{1.69} \right\} \left( 1 - \sqrt{\frac{\rho_x}{\rho_l}} \right) + \sqrt{\frac{\rho_x}{\rho_l}}$ Else $C_o = \left\{ -2.88 \left( \frac{U_{sg}}{U_m} \right) + 4.08 \right\} \left( 1 - \sqrt{\frac{\rho_x}{\rho_l}} \right) + \sqrt{\frac{\rho_x}{\rho_l}}$	$U_{gm} = \sqrt{2} \left( \frac{\sigma g\Delta\rho}{\rho_l^2} \right)^{0.25} (1-\alpha)^{1.75} \exp \left( -1.39 U_{sg} \left( \frac{\sigma g\Delta\rho}{\rho_l^2} \right)^{-0.25} \right)$ $+ (U_{gm}/K_l) \left\{ 1 - \exp \left( -1.39 U_{sg} \left( \frac{\sigma g\Delta\rho}{\rho_l^2} \right)^{-0.25} \right) \right\}$ $(U_{gm}/K_l)$ is the drift velocity given by [56] (Recommended for large pipe diameters in bubbly flow regime)
[44]	For $-20 \leq U_{gm}^* < 0$ where $U_{gm}^* = (U_{gm}/U_m)$ $C_o = (-0.0214 U_{gm}^* + 0.772) + (0.0214 U_{gm}^* + 0.228) \sqrt{\rho_o/\rho_l}$ Else, $C_o = (0.2 \exp(0.00848 U_{gm}^* + 20) + 1) - 0.2 \exp(0.00848 U_{gm}^* + 20) \sqrt{\rho_o/\rho_l}$	$U_{gm} = \sqrt{2} (g\sigma\Delta\rho/\rho_l^2)^{0.25}$

(continued)

**Table 4.2** (continued)

Correlation	Distribution parameter	Drift velocity (m/s)
[57]	For $0 < U_m \leq -3.5$ $C_o = 1.2 - 0.2\sqrt{(\rho_g/\rho_l)}$ For $-3.5 < U_m \leq -2.5$ $C_o = 0.9 + 0.1\sqrt{\rho_g/\rho_l} - 0.3\left(1 - \sqrt{\rho_g/\rho_l}\right)(2.5 + U_m)$ For $-2.5 < U_m < 0$ $C_o = 0.9 + 0.1\sqrt{\rho_g/\rho_l}$ $C_o = 1.185$ (bubbly flow) $C_o = 1.15$ (slug flow)	Refer to [57] to determine drift velocity based on several criteria of mixture velocity, system pressure and pipe diameter
[17]	$C_o = 0.934(1 + 1.42\alpha)$ $C_o = 1.12$	$U_{gm} = 1.53(\sigma g \Delta \rho / \rho_l^2)^{0.25}$ $U_{gm} = 0.35\sqrt{gD(\Delta \rho / \rho_l)}$ $U_{gm} = 1.53(\sigma g \Delta \rho / \rho_l)^{0.25}$ $U_{gm} = 0.345\sqrt{gD(\Delta \rho / \rho_l)}$
[26]	$C_o = 1 + 0.796 \exp(-0.061\sqrt{\rho_l/\rho_g})$	$U_{gm} = 0.034\left(\sqrt{\rho_l/\rho_g} - 1\right)$
[49]	$C_o = 1.08$	0.45
[53]	$C_o = 1$	$U_{gm} = 0.188(gD\Delta \rho / \rho_l)^{0.5}$
Toshiba <sup>b</sup>	$C_o = 1.11775 + 0.45881\alpha - 0.57656\alpha^2$	$U_{gm} = k \frac{C_o(1 - C_o)}{m^2 + C_o \alpha} \left(\sqrt{\rho_g/\rho_l} - m\right) \sqrt{\frac{gD\Delta \rho}{\rho_l}}$
[11]		$k = \sqrt{Ku^2/D^*}$ , $m = 1.36$ ,
[97]		$Ku = \sqrt{\left(D^* \min\left(\frac{1}{2.4}, \frac{10.24}{D^*}\right)\right)}$ , $D^* = D\sqrt{g\Delta \rho / \sigma}$
[56]	For circular pipes $C_o = 1.2 - 0.2\sqrt{(\rho_g/\rho_l)}$ For rectangular pipes $C_o = 1.35 - 0.35\sqrt{(\rho_g/\rho_l)}$	For $N_{jff} \leq 0.00225$ and $D^* \leq 30$ $U_{gm} = 0.0019(D^*)^{0.809} (\rho_g/\rho_l)^{-0.157} N_{jff}^{-0.562} (g\sigma\Delta \rho / \rho_l)^{0.25}$ For $D^* \geq 30$ , $U_{gm} = 0.03(\rho_g/\rho_l)^{-0.157} N_{jff}^{-0.562} (g\sigma\Delta \rho / \rho_l)^{0.25}$ For $N_{jff} > 0.00225$ , $U_{gm} = 0.92(\rho_g/\rho_l)^{-0.157} (g\sigma\Delta \rho / \rho_l)^{0.25}$ $N_{jff} = \left(\mu_l / (\rho_l \sigma \sqrt{g\Delta \rho})^{0.5}\right)$ , $D^* = D / \sqrt{\sigma / g\Delta \rho}$

(continued)

**Table 4.2** (continued)

Correlation	Distribution parameter	Drift velocity (m/s)
[90]	$C_o = 1.2$	$U_{gm} = \left\{ 0.24 + 0.35 (U_{sg}/U_m)^2 \sqrt{gD\alpha} \right\}$
[95]	$C_o = (0.82 + 0.18 P_{3\%} P_{crit})^{-1}$	$U_{gm} = \sqrt{2} (g\sigma\Delta\rho/\rho_l^2)^{0.25}$
[70]	$C_o = 1.3$	$U_{gm} = 0.7$
[59]	$C_o = 1.2$	$U_{gm} = 0.345 \sqrt{gD(\Delta\rho/\rho_l)}$
[15]	$C_o = 1.2$	$U_{gm} = \pm 0.35 \sqrt{gD(\Delta\rho/\rho_l)}$
[112]	$C_o = 1.2 + 0.38 \exp(-1.39/La)$	Drift velocity assumed negligible in mini-channels
[21]	$C_o = \frac{2}{1 + (\text{Re}_v/1000)^2} + \frac{1.2 - 0.2 \sqrt{\rho_g/\rho_l(1 - \exp(-18a))}}{1 + (1000/\text{Re}_v)^2}$	$U_{gm} = 0.0246 \cos \theta + 1.606 \left( \frac{g\sigma\Delta\rho}{\rho_l} \right)^{0.25} \sin \theta$
[25] <sup>c</sup>	$\alpha = \frac{h^*}{1 + (h^* - 1)^{0.6}}$ where, $h = -2.129 + 3.129(\rho^* \rho_l^{-1})^{-0.2186}$ and $n = 0.3487 + 0.6513(\rho_g \rho_l^{-1})^{0.5150}$	

<sup>a</sup> Refer to the original paper for other flow patterns specific correlation each for bubbly, slug, froth, churn and annular flow regime

<sup>b</sup> Reported by Woldesemayat and Ghajar [105]

<sup>c</sup> Not a drift flux model correlation but considered in this chapter since it performs well in high region of void fraction

**Table 4.3** Air-water experimental data used for assessment of void fraction correlations

Data source	D [mm]	Orientation [deg.]	No. of data points	Void fraction range
Two Phase Flow Lab, Oklahoma State University	12.7	0, $\pm 90$	530	0.02–0.93
[79]	5	90	58	0.17–0.96
[55]	19	90	57	0.59–0.96
[2]	50	0	56	0.2–0.69
[31]	–	90	61	0.09–0.92
[32]	60.1	0.5, 1, 3	91	0.35–0.97
[81]	51	1, 0, $-1$ , $-2$	112	0.9–0.98
[5]	78	0	36	0.94–0.99
[22]	75.9	90	103	0.14–0.93
[35]	50.7	90	90	0.03–0.95
[10]	25.4, 38.1	$\pm 90$ , $\pm 85$ , $\pm 75$ , $\pm 35$ , $\pm 20$ , $\pm 15$ , $\pm 10$ , $\pm 5$ , 0	565	0.09–0.99
[76]	44.5	0, 2.75, 20.75, 45, 70, 90, $-6.75$ , $-20.5$ , $-44.5$ , $-67.5$ , $-90$	1521	0.01–0.99
[80]	25.4	$\pm 90$	290	0.05–0.96
[77]	44.5	$\pm 90$	159	0.05–0.92
[29]	32	$-90$	26	0.03–0.29
[82]	19	$-90$	35	0.11–0.95
[50]	50.8	$-90$	39	0.75–0.97
[110]	9.52	$\pm 90$	163	0.06–0.97
[67]	44, 90	$-90$	115	0.01–0.21
[102]	16	$-90$	25	0.07–0.89
[94]	12.7	90	94	0.01–0.98
[61]	48.2	30, 50, 60, 70, 90	460	0.02–0.82
[37]	19	0	88	0.06–0.94
[72]	77.9	0	54	0.54–0.99
[33]	50.8, 149	0	40	0.25–0.91
[106]	4.5	0, 30, 60	123	0.008–0.96
[3]	25.4	90	171	0.6–0.97

**Table 4.4** Refrigerant void fraction data used for assessment of void fraction correlations

Data source	D [mm]	Refrigerant	No. of data points	Void fraction range
[58]	8	R410A	77	0.21–0.99
[89]	0.5, 1.19, 2.96	R410A	142	0.09–0.98
[60]	7.52	R134a	29	0.2–0.98
[109]	4.26	R134a, R410A	36	0.57–0.97
[104]	13.6	R22, R410A	43	0.31–0.98
[16]	7.2	R134a	81	0.35–0.82
[46]	7.04	R410A, R134a	40	0.31–0.95
[87]	9.57	R11, R12, R22	197	0.35–0.99

of void fraction are selected such that they approximately represent different gas-liquid two phase flow patterns. For example, the lowest range of the void fraction approximately represents the bubbly flow regime, the intermediate two ranges of the void fraction represent slug, churn, froth and stratified flow regimes while the last range of void fraction represents annular flow regime. The knowledge of void fraction in two phase flow is usually of no interest unless it is used to calculate other quantities required for process design and sizing of equipment. For example, one of the important uses of void fraction is to calculate the hydrostatic pressure drop based on the correct estimation of two phase mixture density which in turn depends on the correct prediction of the void fraction. Thus the selection of void fraction largely depends upon the desired accuracy or the acceptable error associated with the derived quantities. Ghajar and Bhagwat [41] showed that the void fraction correlation directly influences the two phase mixture density and this influence is of different magnitude for different ranges of the void fraction. They reported that an error of up to  $\pm 30\%$  in small range of void fraction ( $0 < \alpha \leq 0.25$ ) has a small effect on two phase mixture density while a relatively small error of  $\pm 10\%$  in prediction of the large range of void fraction ( $0.75 < \alpha < 1$ ) may cause a considerable error in estimation of the two phase mixture density. Taking into account this relation between error in prediction of the void fraction and its effect of two phase mixture density, an error of up to  $\pm 30\%$  is accepted for the low range of void fraction while an error less than  $\pm 10\%$  is considered acceptable for the highest range of the void fraction. For the two intermediate ranges of the void fraction, an error up to  $\pm 20\%$  is considered acceptable. In past, the work of [43] shortlisted top performing correlations for horizontal, vertical upward and vertical downward flow based on a similar criterion. Their recommendations were based on the percentage of data points predicted within  $\pm 30$ ,  $\pm 20$ ,  $\pm 15$  and  $\pm 10\%$  error bands for four different ranges of the void fraction, respectively. The void fraction data base for air water fluid combination consists of several pipe orientations and hence the assessment of the void fraction correlations is carried out for the above mentioned ranges of the void fraction for seven different classifications of the pipe orientations as shown in Tables 4.5, 4.6, 4.7 and 4.8. In order to select the appropriate correlation from these tables, users may have to solve the top performing correlations on an iterative basis using computer program. To simplify this process, for each void fraction range, corresponding gas volumetric flow fraction range ( $\beta$ ) is also reported in these tables. The gas volumetric flow fraction ( $\beta$ ) defined as the ratio of the superficial velocity of the gas phase to the total two phase (mixture) velocity is known based on the flow rate of each phase. Thus, it is recommended for users to first verify the gas volumetric flow fraction range and then use the appropriate correlation for corresponding void fraction range.

As shown in Table 4.5, for the first two ranges of void fraction in vertical downward pipe orientation, the correlation of [12] predicts the highest number of data points within  $\pm 30$  and  $\pm 20\%$  error bands. For the next two ranges of void fraction i.e.,  $0.5 < \alpha \leq 0.75$  and  $0.75 < \alpha < 1$ , the correlations of [25, 105] give better accuracy than [12] correlation. As pointed out earlier, the correlation of [25] is based on a modeling method in biochemical kinetics and is neither a separated

**Table 4.5** Top performing correlations for vertical upward and downward flow

Void fraction range	$\theta = -90^\circ$		Void fraction range	$\theta = 90^\circ$	
$0 < \alpha \leq 0.25$ (248 data points)	$\pm 30\%$		$0 < \alpha \leq 0.25$ (294 data points)	$\pm 30\%$	
$0 < \beta \leq 0.25$			$0 < \beta \leq 0.45$		
[12]	96		[12]	84	
[21]	96		[86]	89	
[45]	93		[90]	88	
$0.25 < \alpha \leq 0.5$ (127 data points)	$\pm 20\%$		$0.25 < \alpha \leq 0.5$ (253 data points)	$\pm 20\%$	
$0.2 < \beta \leq 0.55$			$0.3 < \beta \leq 0.8$		
[12]	80		[90]	85	
[21]	76		[12]	84	
[20]	76		[52] <sup>a</sup>	83	
$0.5 < \alpha \leq 0.75$ (130 data points)	$\pm 20\%$		$0.5 < \alpha \leq 0.75$ (363 data points)	$\pm 20\%$	
$0.4 < \beta \leq 0.95$			$0.5 < \beta \leq 0.95$		
[12]	76		[52] <sup>1</sup>	95	
[105]	82		[45]	93	
[25]	88		[12]	92	
$0.75 < \alpha < 1$ (370 data points)	$\pm 5\%$	$\pm 10\%$	$0.75 < \alpha < 1$ (517 data points)	$\pm 5\%$	$\pm 10\%$
$0.65 < \beta < 1$			$0.85 < \beta < 1$		
[12]	51	86	[91]	65	88
[105]	62	82	[105]	63	89
[25]	58	76	[25]	70	91

<sup>a</sup> Flow pattern specific correlation for slug flow

flow nor a drift flux model based correlation whereas [105] is a drift flux model based void fraction correlation. For the lowest range of void fraction in vertical upward flow, the correlation of [86] gives best performance and predicts 89 % of data points within  $\pm 30\%$  error bands. The correlation of [12] also gives comparable performance for the first three ranges of void fraction i.e., for  $\alpha \leq 0.75$ . Similar to vertical upward flow, for the last range of void fraction in vertical upward flow [25, 105] are among the top performers.

Based on the pipe orientation, the experimental void fraction data in downward inclined pipe orientations is divided into two categories namely  $0^\circ > \theta \geq -45^\circ$  and  $-45^\circ > \theta > -90^\circ$ . Due to very limited data available in the literature, the entire range of void fraction is divided into three categories i.e.,  $0 < \alpha \leq 0.5$ ,  $0.5 < \alpha \leq 0.75$  and  $0.75 < \alpha < 1$ . As listed in Table 4.6, for  $0^\circ > \theta \geq -45^\circ$ , correlation of [12] is among the top three performing correlations for  $\alpha \leq 0.75$ . For the large values of void fraction, the correlations of [25, 91, 105] are the top performers. In case of pipe orientation in a range of  $-45^\circ > \theta > -90^\circ$ , correlations of [105] consistently stays among the top three performing correlations for every range of void fraction.

Similar to downward inclined pipe orientations, the top performing correlations for the void fraction data in upward inclined pipe orientations are also categorized

**Table 4.6** Top performing correlations for downward inclined pipe orientations

Void fraction range	$0^\circ > \theta \geq -45^\circ$	Void fraction range	$-45^\circ > \theta > -90^\circ$
$0 < \alpha \leq 0.5$ (33 data points)	$\pm 30\%$	$0 < \alpha \leq 0.5$ (15 data points)	$\pm 30\%$
$0 < \beta \leq 0.5$		$0 < \beta \leq 0.4$	
[83]	79	[105]	75
[12]	76	[12]	63
[57]	70	[114]	75
$0.5 < \alpha \leq 0.75$ (59 data points)	$\pm 20\%$	$0.5 < \alpha \leq 0.75$ (18 data points)	$\pm 20\%$
$0.4 < \beta \leq 0.9$		$0.3 < \beta < 0.8$	
[25]	93	[105]	72
[12]	90	[25]	72
[114]	88	[83]	72
$0.75 < \alpha < 1$ (368 data points)	$\pm 5\%$ $\pm 10\%$	$0.75 < \alpha < 1$ (89 data points)	$\pm 5\%$ $\pm 10\%$
$0.8 < \beta < 1$		$0.8 < \beta < 1$	
[105]	66 78	[105]	81 88
[25]	69 81	[19]	83 94
[91]	65 79	[91]	79 88

for two different ranges of the pipe orientations i.e.,  $0^\circ < \theta \leq 45^\circ$  and  $45^\circ < \theta < 90^\circ$  as shown in Table 4.7. Sufficient void fraction data is available for the upward inclined pipe orientation and hence the top performing correlations are presented for all four ranges of the void fraction as discussed before. For both ranges of pipe orientation in upward inclined flow, the correlation of [12] is consistently a top performer for first three ranges of void fraction whereas for the large values of void fraction ( $\alpha > 0.75$ ) [105] gives the best accuracy.

For both ranges of the pipe orientations i.e.,  $0^\circ < \theta \leq -45^\circ$  and  $45^\circ < \theta < 90^\circ$  [12] correlation predicts the highest number of data points for the first three ranges of the void fraction up to  $\alpha \leq 0.75$ . For the highest range of the void fraction i.e.,  $0.75 < \alpha < 1$ , correlation of [105] is observed to give best performance and is followed by the performance of [91] correlation. In case of horizontal two phase flow, limited data is available for the first two ranges of void fraction. As shown in Table 4.8, the correlation of [83] gives best performance for the first two ranges of the void fraction. For the void fraction range of  $0.25 < \alpha \leq 0.5$ , correlation of [105] also gives comparable performance to that of [83]. For the next two ranges of the void fraction i.e.,  $0.5 < \alpha \leq 0.75$  and  $0.75 < \alpha < 1$  [105] gives best accuracy by predicting more than 90 % of data points within  $\pm 20$  and  $\pm 10\%$  error bands, respectively.

In case of refrigerant void fraction data in horizontal two phase flow, the top five performing correlations are presented in Table 4.9. It is observed that the correlation of [105] gives consistent and superior performance in all three ranges of the void fraction. Although the accuracy of [12] correlation is not comparable with the other top performing correlations listed in Table 4.9, it is evident that this correlation gives comparable performance for the first two ranges of the void

**Table 4.7** Top performing correlations for upward inclined pipe orientations

Void fraction range	$0^\circ < \theta \leq 45^\circ$		Void fraction range	$45^\circ < \theta < 90^\circ$	
$0 < \alpha \leq 0.25$ (159 data points)	$\pm 30\%$		$0 < \alpha \leq 0.25$ (283 data points)	$\pm 30\%$	
$0 < \beta \leq 0.85$			$0 < \beta \leq 0.5$		
[12]	84		[12]	85	
[47]	67		[47]	84	
[8]	64		[53]	81	
$0.25 < \alpha \leq 0.5$ (167 data points)	$\pm 20\%$		$0.25 < \alpha \leq 0.5$ (139 data points)	$\pm 20\%$	
$0.3 < \beta \leq 0.95$			$0.3 < \beta \leq 0.8$		
[12]	90		[12]	93	
[105]	87		[47]	83	
[86]	79		[90]	86	
$0.5 < \alpha \leq 0.75$ (158 data points)	$\pm 20\%$		$0.5 < \alpha \leq 0.75$ (104 data points)	$\pm 20\%$	
$0.6 < \beta \leq 0.95$			$0.55 < \beta \leq 0.95$		
[105]	95		[105]	99	
[12]	94		[12]	100	
[52] <sup>a</sup>	98		[90]	100	
$0.75 < \alpha < 1$ (521 data points)	$\pm 5\%$	$\pm 10\%$	$0.75 < \alpha < 1$ (148 data points)	$\pm 5\%$	$\pm 10\%$
$0.9 < \beta < 1$			$0.9 < \beta < 1$		
[105]	83	92	[105]	89	98
[25]	82	96	[12]	70	91
[91]	79	96	[91]	64	89

<sup>a</sup> Flow pattern specific correlation for slug flow

**Table 4.8** Top performing correlations for horizontal pipe orientation

Void fraction range	$\theta = 0^\circ$	
$0 < \alpha \leq 0.25$ (33 data points)	$\pm 30\%$	
$0 < \beta \leq 0.25$		
[12]	76	
[91]	79	
[83]	82	
$0.25 < \alpha \leq 0.5$ (88 data points)	$\pm 20\%$	
$0.2 < \beta \leq 0.5$		
[105]	90	
[19]	91	
[83]	90	
$0.5 < \alpha \leq 0.75$ (183 data points)	$\pm 20\%$	
$0.5 < \beta \leq 0.95$		
[12]	93	
[105]	95	
[86]	95	
$0.75 < \alpha < 1$ (295 data points)	$\pm 5\%$	$\pm 10\%$
$0.95 < \beta < 1$		
[105]	83	99
[25]	74	92
[86]	77	97

**Table 4.9** Top performing correlations for refrigerant vapor two phase flow in horizontal pipe

Void fraction range	$0 < \alpha \leq 0.5$	$0.5 < \alpha \leq 0.75$		$0.75 < \alpha < 1$	
No. of data points	73	184		388	
Correlations	$\pm 30\%$ error bands	$\pm 20\%$	$\pm 30\%$	$\pm 5\%$	$\pm 10\%$
[20]	48	57	62	73	87
[91]	51	54	61	78	88
[7]	53	43	60	59	79
[105]	<b>49</b>	<b>60</b>	<b>62</b>	<b>87</b>	<b>91</b>
[86]	49	54	61	80	88
[12]	45	56	60	28	73

**Table 4.10** Recommended void fraction correlations for different two phase flow situations

$\theta$ [deg]	D [mm]	$\alpha$	$\beta$	Correlation
<i>Air-water data</i>				
-90	9-90	$0 < \alpha \leq 0.5$	$0 < \beta \leq 0.55$	[12]
		$0.5 < \alpha < 1$	$0.45 < \beta < 1$	[105]
90	5-200	$0 < \alpha \leq 0.75$	$0 < \beta \leq 0.95$	[12]
		$0.75 < \alpha < 1$	$0.85 < \beta < 1$	[105]
$-45 \leq \theta < 0$	25-50	$0 < \alpha \leq 0.75$	$0 < \beta \leq 0.9$	[12]
		$0.75 < \alpha < 1$	$0.8 < \beta < 1$	[105]
$-90 < \theta < -45$	25-45.5	$0 < \alpha < 1$	$0 < \beta < 1$	[105]
		$0 < \theta \leq 45$	25-60	$0 < \alpha \leq 0.75$
$45 < \theta < 90$	25-50	$0 < \alpha \leq 0.75$	$0.9 < \beta < 1$	[105]
		$0.75 < \alpha < 1$	$0.9 < \beta < 1$	[105]
0	12.5-149	$0 < \alpha \leq 0.25$	$0 < \beta \leq 0.25$	[83]
		$0.25 < \alpha < 1$	$0.2 < \beta < 1$	[105]
<i>Refrigerant data</i>				
0	0.5-13.6	$0 < \alpha < 1$	$0 < \beta < 1$	[105]

fraction. Overall it is found that for refrigerant two phases flow, even the top performing correlations have limited success in prediction of the void fraction for  $0 < \alpha \leq 0.5$  and  $0.5 < \alpha \leq 0.75$ . For the highest range of the void fraction correlation of [105] gives best accuracy and predicts 87 % of data points within  $\pm 5\%$  error bands. Based on the overall performance of the correlations listed in Table 4.9, it is recommended to use [105] correlation independent of the flow patterns and void fraction range.

The top performing correlations reported in Tables 4.5, 4.6, 4.7, and 4.8, can be used for different ranges of void fraction ( $\alpha$ ) and gas volumetric flow fraction ( $\beta$ ). It is seen that some of these top performing correlations perform consistently for most of the two phase flow conditions. In order to avoid selection and use of different correlations for different ranges of pipe orientation and void fraction, following two correlations are recommended for different two phase flow scenarios. As shown in Table 4.10 [12, 105] correlations can be used to predict void fraction for various ranges of pipe orientations and gas volumetric flow fraction. In case of the near

vertical downward inclined pipe orientations i.e.,  $-90^\circ < \theta < -45^\circ$  (Table 4.6) and two phase flow of refrigerant through horizontal pipes (Table 4.9), the correlation of [105] may be used for the entire range of void fraction and gas volumetric flow fraction. In case the gas volumetric flow fraction overlaps with the two different ranges of the void fraction then it is recommended to calculate the void fraction using both [12, 105] correlations and select the maximum of two values since the [12] correlation comparatively tend to under predict the void fraction. The selection of correct void fraction correlation for such a case is elucidated at the end of this book chapter in form of a solved problem.

## 4.5 Pressure Drop in Gas-Liquid Two Phase Flow

One of the most common requirements for design and sizing of industrial process and equipment is the determination of pressure drop in the system. This section of the chapter will attempt to provide insight about the different two phase flow variables that affect the two phase frictional pressure drop. In addition to this, this section also provides a brief synopsis of some of the existing methodologies available in the literature and their accuracies associated with the prediction of the two phase pressure drop.

The total pressure drop in gas-liquid two phase flow essentially consists of three components namely, hydrostatic, frictional and accelerational pressure drop. As shown in Eq. (4.5), these three components are additive in nature and in order to calculate total pressure drop, each of these components has to be calculated separately. The contribution of each of these components to the total two phase pressure drop depends on the flow pattern, void fraction, pipe diameter, pipe orientation and the type of two phase flow i.e., boiling or non-boiling two phase flow. The hydrostatic component of the two phase pressure drop is due to the pipe elevation and is calculated using two phase mixture density which in turn depends upon the accurate estimation of void fraction. The hydrostatic component of two phase pressure drop can be calculated as shown in Eq. (4.6). The two phase mixture density based on void fraction is calculated as shown in Eq. (4.7).

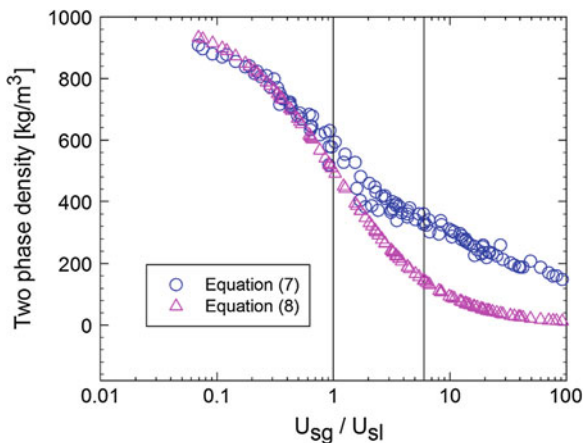
$$\left(\frac{dP}{dL}\right)_{t,tp} = \left(\frac{dP}{dL}\right)_h + \left(\frac{dP}{dL}\right)_f + \left(\frac{dP}{dL}\right)_a \quad (4.5)$$

$$\left(\frac{dP}{dL}\right)_h = \rho_{tp} g \sin \theta \quad (4.6)$$

$$\rho_{tp} = (1 - \alpha)\rho_l + \alpha\rho_g \quad (4.7)$$

In case if the void fraction is not known, two phase flow literature also reports another simple way of calculating two phase mixture density using flow quality as shown in Eq. (4.8). This approach is called a homogeneous flow model approach

**Fig. 4.14** Two phase mixture density as a function of void fraction and flow quality



in which it is assumed that the two phases flow with the same velocity i.e., it assumes no slip between the gas and liquid phase. However, in practise, with an exception of very small region of void fraction (bubbly flow region) there exists a significant slip between the two phases.

$$\rho_{tp} = \left( \frac{x}{\rho_g} + \frac{1-x}{\rho_l} \right)^{-1} \quad (4.8)$$

As shown in Fig. 4.14, the two phase density calculated using void fraction and quality, Eqs. (4.7) and (4.8) are in agreement for the small region of void fraction ( $U_{sg}/U_{sl} \approx 1$ ) but shows a significant discrepancy for annular flow regime ( $U_{sg}/U_{sl} > 1$ ). Thus it can be concluded that the use of homogeneous flow model to predict two phase mixture density may be acceptable only for the small region of void fraction where the slip between the two phases is negligible and in case of considerable slip between the two phases mixture density calculated by Eq. (4.7) should be preferred. The data plotted in Fig. 4.14 is for air water fluid combination measured at Two Phase Flow Lab, Oklahoma State University. Similar interaction between Eqs. (4.7) and (4.8) is expected for different fluid combinations.

The accelerational component of two phase pressure drop is due to the expansion of gas phase as the two phase mixture travels downstream and is trivial for non-boiling two phase flow and hence can be neglected. However, in case of boiling two phase flow; the pressure drop due to acceleration of the gas phase can offer a significant contribution to the total pressure drop depending upon the pipe diameter and pipe orientation. It should be noted that similar to hydrostatic component, the calculation of accelerational component of two phase pressure drop also requires correct estimation of void fraction at pipe inlet and exit flow conditions. The frictional component of two phase pressure drop is essentially due to the friction at pipe wall and gas-liquid interface and is the most complex and

difficult to predict due to its dependency on several parameters such as, pipe orientation, surface roughness, pipe geometry, fluid properties, and flow patterns. The accelerational and frictional pressure drop components are expressed by Eqs. (4.9) and (4.10), respectively.

$$\left(\frac{dP}{dL}\right)_a = \frac{1}{L} \left\{ \left[ \frac{G_l^2}{\rho_l(1-\alpha)} + \frac{G_g^2}{\rho_g\alpha} \right]_{out} - \left[ \frac{G_l^2}{\rho_l(1-\alpha)} + \frac{G_g^2}{\rho_g\alpha} \right]_{in} \right\} \quad (4.9)$$

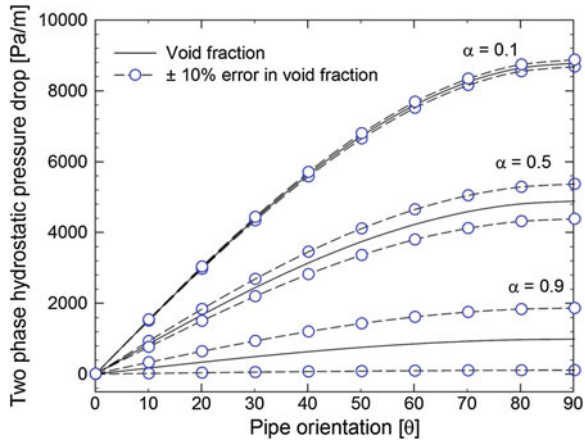
$$\left(\frac{dP}{dL}\right)_{tp,f} = \frac{f_{tp} G^2}{2D\rho_p} \quad (4.10)$$

## 4.6 Void Fraction and Hydrostatic Pressure Drop

As mentioned earlier, the direct influence of the void fraction on two phase hydrostatic pressure drop is through the mixture density and hence it is important to understand the sensitivity of two phase hydrostatic pressure drop to the void fraction. The two phase mixture density given by Eq. (4.7) is of weighted nature and is found to be sensitive to the large values of void fraction compared to the small values of void fraction. From Eq. (4.6), it is clear that the effect of error in void fraction on the calculation of hydrostatic pressure drop is maximum for vertical pipe orientation. As shown in Fig. 4.15, two phase hydrostatic pressure drop is more sensitive to the error in void fraction for the large values of void fraction in vertical pipe orientation. Whereas, the same error of  $\pm 10\%$  in low region of void fraction virtually doesn't influence the hydrostatic pressure drop. Since, the total pressure drop is of additive nature, it is desired to keep the error in each of these components as low as possible. In order to achieve this accuracy, it is required to have a correlation that will predict the void fraction with a minimum error for the large values of void fraction (annular flow). The correlation of [105] presented in the previous section satisfies this condition and is hence recommended for use for high values of void fraction.

It is also worthwhile to mention that the effect of error in void fraction on two phase hydrostatic pressure drop and hence on the overall accuracy in calculation of total two phase pressure drop may worsen in case of large pipe diameters. For small diameter pipes, compared to the hydrostatic pressure drop usually the frictional pressure drop has a greater share to the total two phase pressure drop and hence any error induced in hydrostatic pressure drop due to the error in void fraction is damped out. However, with increase in the pipe diameter, the share of hydrostatic pressure drop to the total two phase pressure drop becomes considerable and hence noticeably contributes to the total error. A better illustration of this scenario is reported by Ghajar and Bhagwat [41].

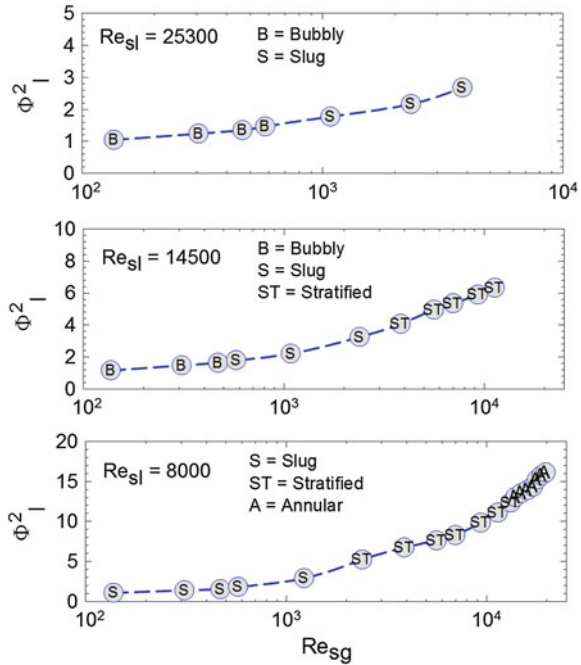
**Fig. 4.15** Effect of void fraction error on two phase hydrostatic pressure drop (Eq. 4.6) for different pipe orientations



#### 4.6.1 Effect of Flow Patterns and Pipe Diameter on Two Phase Frictional Pressure Drop

The frictional pressure drop in gas liquid two phase flow is essentially due to the friction of liquid or gas phase at the pipe wall and the friction at gas liquid interface. The relative magnitudes of the friction at pipe wall and at the gas liquid interface depend on the physical structure of individual flow patterns. For instance, the contribution of the interfacial friction to the two phase frictional pressure drop is significant when there is significant slippage between the two phases as in case of stratified and annular flow regimes. On the other hand, the gas liquid interfacial friction is trivial when the one phase is dispersed in another continuous phase and hence there is negligible slippage between the two phases as in case of bubbly flow regime. Consequently, the two phase frictional pressure drop in bubbly flow regime is mostly due to the friction of single phase liquid at the pipe wall and hence magnitude wise is only about 1–2 times higher than that of single phase flow. These higher magnitudes of two phase pressure drop in bubbly flow regime (small region of void fraction), are due to the turbulent eddies and the disturbances created in continuous liquid medium by the dispersed bubbles. For the other extreme of the two phase flow regime i.e., annular flow (separated flow), the magnitude of the interfacial friction is very high causing the two phase frictional pressure drop to be significantly higher (up to 1000 times depending upon the pipe diameter) than the corresponding single phase pressure drop measured at equivalent mass flow rates. The relationship between the two phase frictional pressure drop in terms of two phase frictional multiplier with the flow patterns in horizontal pipe orientation is evident from Fig. 4.16. The two phase frictional multiplier ( $\Phi_f^2$ ) is the ratio of the two phase frictional pressure drop to the pressure drop of single phase liquid or gas when assumed to flow through the pipe. The different forms of two phase frictional multiplier are discussed later in this work. It is observed that

**Fig. 4.16** Two phase frictional pressure drop for different flow patterns in horizontal pipe orientation (air-water fluid combination)



for the two phase pressure drop data measured in a 12.5 mm I.D. pipe using air-water fluid combination, the two phase frictional multiplier is close to unity for bubbly flow while is about 10–15 for annular flow regime. Similar relationship between the two phase frictional multiplier and the flow patterns exists for different pipe orientations and fluid combinations.

Similar to the single phase pressure drop, the frictional pressure drop in gas-liquid two phase flow is inversely proportional to the pipe diameter. However, as shown in the previous sections, the effect of pipe diameter on two phase frictional pressure drop at fixed pipe orientation is of different magnitude for different two phase flow regimes. It is found that the two phase frictional pressure drop in annular flow regime depends upon the pipe diameter to a great extent whereas it is relatively less sensitive to the pipe diameter in bubbly flow regime. As shown in Fig. 4.17, it is clear that for horizontal two phase flow at fixed mass flow rate of R134a, the two phase frictional pressure drop for different pipe diameters deviates significantly for large values of flow quality (annular flow regime) whereas, for low mass qualities, the pipe diameter has little effect on two phase frictional pressure drop. Similar conclusions were drawn from the work of [55] who compared the two phase frictional pressure drop of air-water in vertical upward flow for pipe diameters in a range of  $10 \text{ mm} < D < 50 \text{ mm}$ . As mentioned earlier, the frictional pressure drop is due to the friction at pipe wall and friction at gas-liquid interface. The gas liquid interfacial area increases with increase in the pipe diameter and thus although the total two phase frictional pressure drop for larger

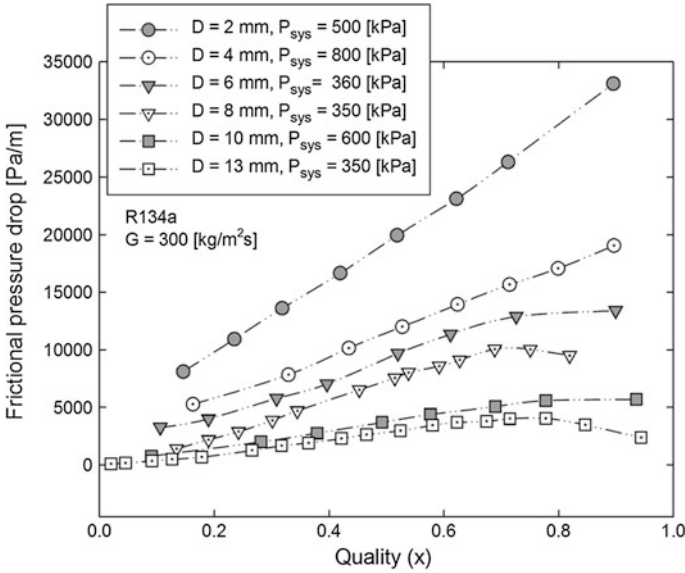


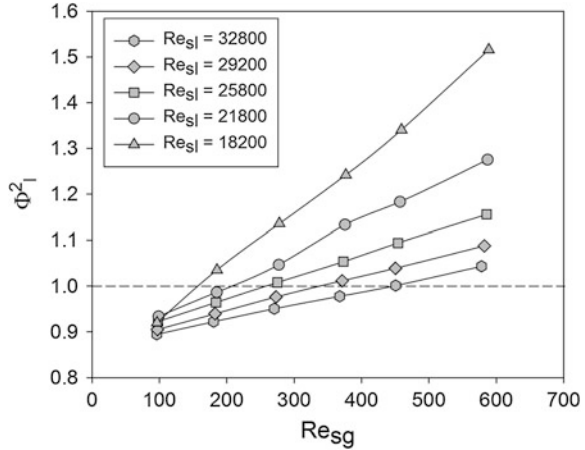
**Fig. 4.17** Effect of pipe diameter on two phase frictional pressure drop in horizontal pipe orientation

pipe diameters is less than that compared to the smaller pipe diameters, the two phase frictional multiplier for large diameter pipes may be greater than that for the relatively smaller diameter pipes. Thus it is evident that any correlation developed to predict two phase frictional pressure drop must account for the pipe diameter effect in the high quality region or alternatively the annular flow regime.

### 4.6.2 Effect of Pipe Orientation on Two Phase Frictional Pressure Drop

In addition to the flow patterns and pipe diameter, the pipe orientation is also found to influence the two phase frictional pressure drop. For vertical two phase flow, the effect of pipe orientation on two phase frictional pressure drop is observed in vertical downward bubbly flow in form of coring phenomenon. This effect can be very well illustrated by presenting the measured two phase frictional pressure drop in form of two phase frictional multiplier [introduced later through Eq. (4.14)]. As shown in Fig. 4.18, for air-water vertical downward bubbly flow, the non-dimensional pressure drop in form of two phase frictional multiplier ( $\Phi_l^2$ ) is initially less than unity and then increases with increase in the gas superficial Reynolds number. This means that at the onset of bubbly flow the two phase

**Fig. 4.18** Non-dimensional two phase frictional pressure drop in vertical downward bubbly flow (air-water data in 12.5 mm I.D. pipe)



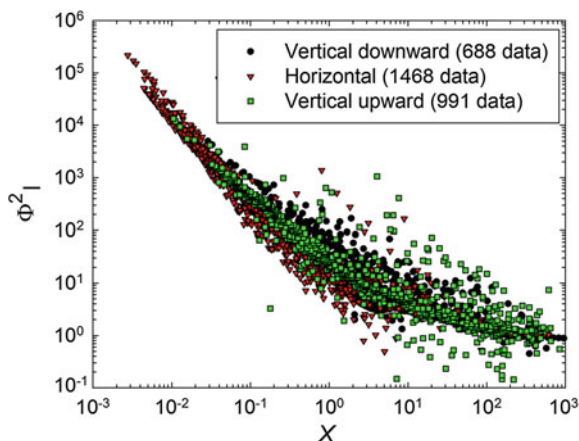
frictional pressure drop is less than the single phase pressure drop calculated using Eq. (4.12). This trend in the data is essentially due to the coring phenomenon mentioned earlier in the section of flow patterns. With increase in both gas and liquid flow rates, the coring phenomenon gradually goes away and the two phase frictional pressure drop becomes higher than the single phase pressure drop yielding  $\Phi_1^2$  greater than unity. This phenomenon is not observed in the vertical upward and horizontal flow and hence the two phase frictional pressure drop increases with increase in the gas flow rate and is always greater than unity. Due to the lack of data in the literature, the trend of the two phase pressure drop in vertical downward flow and the existence of the coring phenomenon for different fluid combinations could not be verified.

Due to limited information on the flow patterns associated with the two phase pressure drop data, it is difficult to compare the effect of pipe orientation on two phase pressure drop for each flow pattern. However, the graphical representation of the variation of two phase frictional multiplier with respect to the Lockhart-Martinelli parameter [66] gives enough idea about the effect of pipe orientation on two phase frictional pressure drop. The Lockhart-Martinelli parameter is essentially the ratio of single phase liquid and gas frictional pressure drop as expressed by Eq. (4.11).

$$X = \sqrt{(dP/dL)_l / (dP/dL)_g} \tag{4.11}$$

The single phase pressure drop of liquid and gas phase is found using Eqs. (4.14) and (4.15). Thus from the structure of Eq. (4.11) it is evident that the low values of  $X$  represent the annular flow regime while the large values of  $X$  indicate existence of bubbly flow regime. The intermediate values of  $X$  are occupied by slug, stratified, froth and churn flow regimes. As shown in Fig. 4.19,

**Fig. 4.19** Two phase frictional multiplier as a function of Lockhart-Martinelli parameter [66] for different pipe orientations (air-water data)



the large scatter for  $X > 0.1$  indicates that the effect of pipe orientation is significant for non-annular flow patterns (buoyancy and gravity effect dominated flow). For  $X < 0.1$  typically the annular flow regime (inertia effect dominated flow), the effect of pipe orientation on two phase frictional pressure drop gradually goes away. Some of the data for vertical upward pipe orientation that assumes the two phase frictional multiplier values less than unity are essentially due to the flow reversal phenomenon mostly observed for the churn flow regime. The flow reversal in churn flow regime is associated with the interfacial shear between the gas and liquid phase and the shear stress exerted by the liquid phase on pipe wall. For the sake of brevity the details of the flow reversal and its effect on two phase frictional pressure drop is not included in this chapter. Readers are advised to refer to the comprehensive work of [51, 68] for more details.

Due to the limited data available in the literature for different pipe diameters and orientations, it is difficult to extract the information about the combined effect of pipe orientation and the pipe diameter. However, based on the flow physics and the fact that there exist both buoyancy dominated and inertia dominated two phase flow regimes, it can be speculated that the effect of pipe orientation on two phase frictional pressure drop in buoyancy driven flows is more pronounced for large pipe diameters compared to the small diameter pipes. The two phase frictional pressure drop data shown in Fig. 4.19, is for air-water fluid combination and consists of a range of pipe diameters,  $12.5 \text{ mm} < D < 152 \text{ mm}$ ,  $9.5 \text{ mm} < D < 50 \text{ mm}$  and  $12.5 \text{ mm} < D < 45.5 \text{ mm}$  for horizontal, vertical upward and vertical downward flows, respectively. Thus the general trend of the data in Fig. 4.19 for small values of  $X$  gives enough evidence that the two phase frictional pressure drop in annular flow regime is relatively insensitive to the combined effect of pipe orientation and pipe diameter. Similar relationship between the two phase frictional multiplier and the Lockhart-Martinelli parameter is expected for other fluid combinations.

## 4.7 Review of Two Phase Frictional Pressure Drop Correlations

The prediction of two phase hydrostatic and accelerational pressure drop relies on the correct estimation of void fraction whereas the determination of frictional pressure drop in gas liquid two phase flow is much more complex. The two phase frictional pressure drop is determined either by finding a two phase friction factor (homogeneous flow model) or a two phase friction multiplier (separated flow model). These two ways of finding two phase frictional pressure drop are described below.

### 4.7.1 Homogeneous Flow Model Approach

The homogeneous flow model (HFM) assumes the two phases to be well mixed with each other and move with identical velocity (no interfacial slip). Thus in the homogeneous model the underlying idea is to represent the two phase mixture to behave as a pseudo single phase fluid that has fluid properties as that of two phase mixture. Thus HFM can be used with sufficient accuracy only when there is no rapid change in the flow variables and when there is negligible slip between the two phases.

The frictional pressure drop using homogeneous flow model is calculated with conventional equations used for single phase flow using pseudo mixture properties. For single phase flow, the frictional pressure drop is calculated using generalized equation of following form,

$$\left(\frac{dP}{dL}\right)_j = \frac{f_j G^2}{2D\rho_j} \quad (4.12)$$

Most of the homogeneous flow model based two phase frictional pressure drop correlations (two phase dynamic viscosity models listed in Table 4.11) recommend use of [14] correlation to determine friction factor.

$$f_j = 64/Re_j \text{ for laminar flow } (Re_j < 2000)$$

$$f_j = 0.316/Re_j^{0.25} \text{ for turbulent flow } (Re_j > 2000)$$

The subscript 'j' represents gas or liquid phase. This general form of the frictional pressure drop equation can be used to calculate two phase frictional pressure drop using two phase friction factor based on the two phase Reynolds number and the two phase mixture density as shown in Eq. (4.8). The two phase Reynolds number ( $Re_m$ ) is based on the two phase viscosity ( $\mu_m$ ) defined by Eq. (4.13).

$$Re_m = \frac{GD}{\mu_m} \quad (4.13)$$

**Table 4.11** Two phase dynamic viscosity models

Correlation	Expression for two phase dynamic viscosity
[1]	$\mu_m = \mu_l / \left( (1-x) + x\sqrt{\rho_l/\rho_g} \right)$
[9] <sup>a</sup>	$\mu_m = \mu_l(1-\beta)(1+2.5\beta) + \mu_g\beta$
[24]	$\mu_m = x\mu_g + (1-x)\mu_l$
[28]	$\mu_m = \mu_l(1+x(\rho_l/\rho_g-1))$
[30]	$\mu_m = \rho_m(x(\mu_g/\rho_g) + (1-x)(\mu_l/\rho_l))$
[36]	$\mu_m = (1-\beta)\mu_l + \beta\mu_g + 2\sqrt{\beta(1-\beta)\mu_l\mu_g}$
[40]	$\mu_m = (\mu_l\rho_g/x\rho_l + (1-x)\rho_g)$
[64]	$\mu_m = \mu_l\mu_g/\mu_g + x^{1.4}(\mu_l - \mu_g)$
[71]	$\mu_m = (x/\mu_g + (1-x)/\mu_l)^{-1}$
[78]	$\mu_m = (\mu_l(1-\beta) + \mu_g\alpha/(1-\beta+\alpha))$
[4] (Model 1) <sup>b</sup>	$\mu_m = \mu_l \frac{2\mu_l + \mu_g - 2(\mu_l - \mu_g)x}{2\mu_l + \mu_g + (\mu_l - \mu_g)x}$
[4] (Model 2) <sup>b</sup>	$\mu_m = \mu_g \frac{2\mu_g + \mu_l - 2(\mu_g - \mu_l)(1-x)}{2\mu_g + \mu_l + (\mu_g - \mu_l)(1-x)}$
[4] (Model 3) <sup>b</sup>	Arithmetic mean of Model 1 and Model 2
[4] (Model 4) <sup>b</sup>	$\mu_m = \frac{1}{4} \left( \begin{aligned} &(3x-1)\mu_g + [3(1-x)-1]\mu_l \\ &+ \sqrt{[(3x-1)\mu_g + (3\{1-x\}-1)\mu_l]^2 + 8\mu_g\mu_l} \end{aligned} \right)$

<sup>a</sup> Uses [27] friction factor correlation

<sup>b</sup> Uses [23] friction factor correlation

Thus to predict the two phase frictional pressure drop correctly, an appropriate estimate of two phase Reynolds number and hence the two phase dynamic viscosity is obviously required. Literature reports several models to calculate the two phase dynamic viscosity as reported in Table 4.11.

### 4.7.2 Separated Flow Model Approach

Separated flow model accounts for the two phases flowing separately with different velocities and sharing a definite interface between them. Analytical solution to the separated flow model requires in all six equations; mass, momentum and energy conservation equations for each phase. Additional information such as velocity and temperature profile and other hydrodynamic parameters are required to solve these equations thus making it complex and difficult. An easy and a quick approach is to use empirical methods based on extensive experimental data.

The empirical model based on the concept of separated flow was first conceived by Lockhart and Martinelli [66] and since then several investigators have proposed different correlations by modifying the correlation of [66]. The separated flow

model can be expressed in four different ways in terms of the two phase friction multiplier that accounts for the pressure drop due to the flow of single phase liquid or gas. The subscripts 'lo' and 'go' correspond to frictional pressure drop when the single phase liquid or gas flow rate is assumed to be equivalent to the entire two phase mixture flow rate ( $G$ ). Whereas, the subscripts 'l' and 'g' indicate the frictional pressure drop when single phase liquid or gas is flowing at a rate of  $G(1-x)$  and  $Gx$ , respectively. The understanding of these four approaches that can be used in separated flow model becomes more apparent from their mathematical definitions presented by Eqs. (4.14) to (4.17).

$$\left(\frac{dP}{dL}\right)_{tp,f} = \Phi_l^2 \left(\frac{dP}{dL}\right)_l \quad \text{where} \quad \left(\frac{dP}{dL}\right)_l = \frac{f_l G^2 (1-x)^2}{2D\rho_l} \quad (4.14)$$

$$\left(\frac{dP}{dL}\right)_{tp,f} = \Phi_g^2 \left(\frac{dP}{dL}\right)_g \quad \text{where} \quad \left(\frac{dP}{dL}\right)_g = \frac{f_g G^2 x^2}{2D\rho_g} \quad (4.15)$$

$$\left(\frac{dP}{dL}\right)_{tp,f} = \Phi_{lo}^2 \left(\frac{dP}{dL}\right)_{lo} \quad \text{where} \quad \left(\frac{dP}{dL}\right)_{lo} = \frac{f_{lo} G^2}{2D\rho_l} \quad (4.16)$$

$$\left(\frac{dP}{dL}\right)_{tp,f} = \Phi_{go}^2 \left(\frac{dP}{dL}\right)_{go} \quad \text{where} \quad \left(\frac{dP}{dL}\right)_{go} = \frac{f_{go} G^2}{2D\rho_g} \quad (4.17)$$

Literature provides several correlations to determine the two phase frictional multipliers as shown in the above equations to predict two phase frictional pressure drop. The two phase frictional pressure drop correlations based on separated flow models are listed in Table 4.12. Most of these correlations are based on Eqs. (4.14) and (4.16) and require the single phase friction factor to be determined using [14] correlation. Any other single phase friction factor correlation recommended by certain correlation is also listed in Table 4.12.

## 4.8 Assessment of Two Phase Frictional Pressure Drop Correlations

The performance of the two phase frictional pressure drop correlations based on homogeneous and separated flow model considered in Tables 4.11 and 4.12 is assessed against a comprehensive data of air water and liquid refrigerant and its vapor consisting of 3147 and 1685 data points, respectively. The air water data consists of horizontal, vertical upward and downward pipe orientations while the refrigerant liquid vapor data consists of horizontal pipe orientation only. The experimental data used for the performance assessment of two phase frictional pressure drop correlations against air-water and refrigerant liquid-vapor is summarized in Tables 4.13.

**Table 4.12** Two phase frictional pressure drop correlations based on separated flow model

Source	Correlation	Comments
[66]	$\Phi_{lo}^2 = 1 + \frac{C}{X} + \frac{1}{X^2}$ where $C = 5, 10, 12$ and $20$ for laminar-laminar, laminar-turbulent, turbulent-laminar and turbulent-turbulent single phase flow conditions, respectively	Developed for data in horizontal smooth pipes
[6]	$\Phi_{lo}^2 = \left( \frac{1-x}{1-x} \right) \left( 1 - \Gamma_{Bf} \left( 1 - \frac{\rho_x}{\rho_l} \right)^{0.43} \left( 1 + x \left( \frac{\rho_x}{\rho_l} - 1 \right) \right)^{1.75} \right)$ where $\Gamma_{Bf} = \left( \frac{0.71 + 2.35(\rho_g/\rho_l)}{1 + (\frac{1-x}{x})(\rho_g/\rho_l)} \right)$	Mathematical representation of the frictional pressure drop given by Barcozy [7]
[18]	$\Phi_{lo}^2 = A_{Fr} + \frac{1.262x^{0.6978}}{We_{lo}^{0.1538}} \left( \frac{\mu}{\rho_g} \right)^{0.3278} \left( \frac{\mu_g}{\mu_l} \right)^{-1.181} \left( 1 - \frac{\mu_x}{\mu_l} \right)^{3.477}$ where $A_{Fr} = (1-x)^2 + x^2 \frac{\rho_l \rho_{g0}}{\rho_g \rho_{l0}}$	Based on condensation of halogenated refrigerants inside a horizontal tube
[20]	$\Phi_{lo}^2 = 1 + (Y^2 - 1)(B_{Ch}x^{1-0.5n}) \left( 1 - x^{(1-0.5n)} \right) + x^{(2-n)}$ where $n = 0.25$ and $Y = \sqrt{(dP/dL)_{go}/(dP/dL)_{lo}}$ , and $B_{Ch}$ is defined based on the combined criteria of mass flux and $Y$ values as reported by Chisholm [20]	Accounts for the variation in two phase frictional pressure drop for different mass flux
[38, 39]	$\text{(For } \theta = 0^\circ \text{ and } +90^\circ) \Phi_{lo}^2 = A_{Fr} + \frac{3.24x^{0.78}(1-x)^{0.22}(\rho_l/\rho_g)^{0.91}(\mu_g/\mu_l)^{0.19}(1-(\mu_g/\mu_l))^{0.7}}{Fr_{lo}^{0.085}We_{lo}^{0.035}}$ $\text{(For } \theta = -90^\circ) \Phi_{lo}^2 = A_{Fr} + \frac{5.7x^{0.7}(1-x)^{0.14}(\rho_l/\rho_g)^{0.88}(\mu_g/\mu_l)^{0.36}(1-(\mu_g/\mu_l))^{0.2}}{Fr_{lo}^{0.09}We_{lo}^{0.007}}$	Based on experimental data bank of 25000 data points for air-water and refrigerants
[48]	$f_{lo} = 0.25 \left[ 0.86859 \ln \left( \frac{Re_g}{1.964 \ln Re_g - 3.8215} \right) \right]^{-2}$ $\Phi_{lo}^2 = 1 + dP_{Fr} \left[ \frac{(\rho_l/\rho_g)}{1 + (\mu_l/\mu_g)^{0.225}} - 1 \right]$ where $dP_{Fr}$ is same as that of [18] except that the single phase friction factors are calculated using $f_{lo} = f(Fr)$ as given by Gronnerud [48]	

(continued)

Table 4.12 (continued)

Source	Correlation	Comments
[75]	$\Phi_{lo}^2 = Y^2 x^3 + (1-x)^{0.33} (1 + 2x(Y^2 - 1)),$ where Y is same as that of [20]	Extrapolation between all liquid and all gas flow Applicable for turbulent-turbulent region and based on flow of refrigerants in horizontal tube
[54]	$\Phi_{lo}^2 = 30.78x^{1.323}(1-x)^{0.477} P_r^{-0.7232}$ where $P_r$ is the reduced pressure of given refrigerant.	
[73]	$\Phi_l^2 = 1 + \frac{C}{X_u} + \frac{1}{X_u^2}$ where $C = 21(1 - \exp(-0.319D))$ Pipe diameter is in [mm]	Based on air-water and refrigerant data. Accounts for pipe diameter effect
[96]	$\Phi_l^2 = 1 + C/X_u^{1.19} + 1/X_u^2$ where, $C = 1.79(\text{Re}_g/\text{Re}_l)^{0.4} ((1/x) - 1)^{0.5}$	Based on more than 2000 data for refrigerants and air-water fluid combinations and $D < 13$ mm
[103]	$\Phi_l^2 = 1 + C/X_u + 1/X_u^2$ where, $C = 4.566 \times 10^{-6} X^{0.128} \text{Re}_{lo}^{0.938} (\rho_g/\rho_l)^{2.15} (\mu_l/\mu_g)^{5.1}$	Based on refrigerant data in 6.5 mm horizontal pipe. Applicable for $50 < G < 700$ kg/m <sup>2</sup> s
[92]	$\Phi_{lo}^2 = 1 + (F^2 - 1)x^{1.75} (1 + 0.952\Gamma X_u^{0.142})$ where, $\Gamma = \sqrt{\rho_l/\rho_g} (\mu_g/\mu_l)^{0.125}$	Based on experimental data of R12, R22, R134a and R32/R125 in horizontal pipe of $D < 10$ mm
[62]	$\Phi_{lo}^2 = 1.7 + \left( (6.3 + F_{r_{lo}})^{0.89} / 1.04 F_{r_{lo}}^{0.52} W_{e_{lo}}^{-0.011} \right) (1/X_u)^{0.42}$	Based on data for R134a and R123 refrigerants in 10 mm I.D. horizontal pipe
[63]	$\Phi_{lo}^2 = \frac{0.36(0.6 + AF_{r_{lp}})}{F_{r_{lp}}^{0.51} W_{e_m}^{-0.031}} X_u^{0.15}$ where $F_{r_{lp}} = (G^2/gD\rho_m^2)$ and $W_{e_{lp}} = (G^2D/\sigma\rho_m)$ and $\rho_m$ is from Eq. (4.8)	

A is variable defined for two different ranges of mixture mass flux

(continued)

Table 4.12 (continued)

Source	Correlation	Comments
[107]	$\Phi_{lo}^2 = \left\{ Y^2 x^3 + (1-x)^{0.33} (1+2x(Y^2-1)) \right\} \left[ 1 + 1.54(1-x)^{0.5} La \right]$ <p>where <math>La</math> is the Laplace constant defined as <math>La = \left( \sqrt{\sigma/g(\rho_l - \rho_g)} / D \right)</math>  <math>Y</math> is same as that of (Chisholm [20]) but the single phase friction factor is calculated using [34]                      correlation</p>	Based on 2600 data of 15 refrigerants for $0.8 < D < 19$ mm in horizontal flow
[111]	$\Phi_{lo}^2 = 1 + 4.2(Y^2 - 1) \left\{ \frac{\beta}{We} x^{0.875} (1-x)^{0.875} + x^{1.75} \right\},$ <p>where <math>Y</math> is same as that of [20]</p>	Modification of [20] correlation. Developed for boiling CO <sub>2</sub> two phase flow in a 7.5 mm horizontal pipe and claims to predict the data within ±20 % error bands
[99]	$\Phi_{lo}^2 = 1 + (4.3Y^2 - 1)La \left\{ x(1-x)^{0.875} + x^{1.75} \right\},$ <p>where <math>Y</math> is same as that of [20]                      and <math>La</math> is the Laplace number used by Xu and Fang [107]</p>	Applicable for R12, R134a and R113 in smooth tubes with $P_{sys} < 860$ kPa
[100]	$\Phi_{lo}^2 = 1 + \frac{C}{X} + \frac{1}{X^2}$ <p>where <math>C = 1.279 \times 10^{-9} A^{-1.96} \Psi Re_{lo}^{0.4}</math> for <math>We_{go} \leq We_{lo}^{0.14}</math> Else  <math>C = 1.386 \times 10^{-4} A^{-0.65} \Psi^{0.2} Re_{lo}^{0.52}</math> where <math>\Psi = \frac{\mu}{\sigma} 1.2 \left( \frac{G_x}{\rho_g} + \frac{G_l}{\rho_l} \right)</math> and <math>A = \mu_l^2 / \rho_l \sigma D^2</math></p>	
[88]	$\Phi_{lo}^2 = 0.38 Re_{lo}^{0.1} \left( 1 + \frac{x}{1-x} \frac{U_x}{U_l} \right)^{0.95}$	Developed for boiling two phase flow of steam-water mixtures in horizontal pipes
[69]	$\Phi_{lo}^2 = \Phi_7^2 (1-x)^{1.75}$ <p>where <math>\Phi_7^2</math> is obtained from [66]</p>	
[112]	$\Phi_l^2 = 1 + C/X_l^{1.19} + 1/X_l^2$ <p>where <math>C = 21(1 - \exp(-C_l/La))</math> and <math>C_l = 0.142</math> and <math>0.674</math> for adiabatic liquid vapor and liquid and gas flow, respectively. <math>La</math> is the Laplace constant used by Xu and Fang [107]</p>	Based on air-water and refrigerant data in horizontal and vertical upward mini and micro channels

**Table 4.13** Summary of experimental data<sup>a</sup> used for performance assessment of two phase frictional pressure drop correlations

Parameter	Range
<i>Air-water (1468 data points) (<math>\theta = 0^\circ</math>)</i>	
Diameter (mm)	12.5–152
Pressure (kPa)	108–680
Mass flux (kg/m <sup>2</sup> s)	1.2–2620
Quality	0.0001–0.99
Void fraction	0.05–0.99
<i>Air-water (991 data points) (<math>\theta = 90^\circ</math>)</i>	
Diameter (mm)	9.5–50
Pressure (kPa)	102–675
Mass flux (kg/m <sup>2</sup> s)	1.1–3260
Quality	0.0001–0.93
Void fraction	0.03–0.99
<i>Air-water (688 data points) (<math>\theta = -90^\circ</math>)</i>	
Diameter (mm)	12.5–45.5
Pressure (kPa)	102–280
Mass flux (kg/m <sup>2</sup> s)	25–2450
Quality	0.0005–0.79
Void fraction	0.02–0.98
<i>Refrigerant (1685 data points) (<math>\theta = 0^\circ</math>)</i>	
Diameter (mm)	1.4–13.8
Pressure (kPa)	150–2650
Mass flux (kg/m <sup>2</sup> s)	25–1082
Quality	0.01–0.97
Void fraction	0.26–0.98
Fluids	CO <sub>2</sub> , R12, R123, R134a, R22, R404a, R407C, R401A, R507

<sup>a</sup> Sources of the experimental data are not reported due to space constraints

The performance of frictional pressure drop correlations considered in this chapter is assessed based on the percentage of data points predicted within  $\pm 30\%$  error bands. The accuracy criteria of  $\pm 30\%$  is based on the overall performance of the correlations and is consistent with the assessment done by other investigators such as [84, 85, 96, 103 (used  $\pm 50\%$ )] and (Xu et al. [108]). The two phase pressure drop data for air water is divided into different ranges of the pipe diameter for each pipe orientation. The assessment of the frictional pressure drop correlations based on this classification gives an impression about their scope to account for the effect of pipe diameter on two phase frictional pressure drop. As shown in Table 4.14, the top performing correlations are short listed for the two phase frictional pressure drop data divided into four categories of the pipe diameter range. For the horizontal two phase flow and smallest pipe diameter of  $D = 12.5$  mm [75] give best accuracy by predicting about 98 % of data within

**Table 4.14** Top performing frictional pressure drop correlations for air-water two phase flow in horizontal pipe orientation

Diameter [mm]	Correlation	% of data within $\pm 30$ % error bands
D = 12.5	[75]	97.9
	[63]	95.4
	[4] (Model 2)	97.1
12.5 < D < 25	[73]	73.2
	[96]	73.2
	[9]	65.4
25 < D < 50	[73]	79.3
	[30]	78.5
	[9]	76.4
90 < D < 150	[73]	63.1
	[30]	66.5
	[9]	67.5

**Table 4.15** Top performing frictional pressure drop correlations for air water two phase flow in vertical upward pipe orientation

Diameter [mm]	Correlation	% of data within $\pm 30$ % error bands
9 < D < 15	[69]	85.4
	[75]	82.3
	[4] (Model 2)	82.1
20 < D < 40	[73]	73.8
	[96]	73.8
	[9]	70.3
40 < D < 50	[38]	70.1
	[75]	66.2
	[4] (Model 3)	68.1

$\pm 30$  % error bands. For the next three ranges of pipe diameter, the correlations of [9, 73] give consistent performance. The correlation of [73] is based on the concept of separated flow model while the correlation of [9] is essentially to predict two phase dynamic viscosity and hence is based on the concept of homogeneous two phase flow model. Overall it is observed that the performance of the both types of two phase frictional pressure drop correlations deteriorate with increase in the pipe diameter. A more detailed look at the performance of these correlations showed that the accuracy of these correlations decrease in particular for the annular flow regime. This is probably because, these correlations do not have enough versatility to account for the increase in the interfacial friction in the annular regime with increase in the pipe diameter.

In case of vertical upward flow, for the lowest range of pipe diameter [69] give best performance by predicting more than 85 % of data within  $\pm 30$  % error bands as shown in Table 4.15. For the intermediate range of pipe diameter i.e., 20 mm < D < 40 mm the correlation of [73] is one of the best correlations that predicts about 74 % of data within  $\pm 30$  % error bands. Similar to the horizontal

**Table 4.16** Top performing frictional pressure drop correlations for air water two phase flow in vertical downward pipe orientation

Diameter [mm]	Correlation	% of data within $\pm 30$ % error bands
10 < D < 20	[18]	76.8
	[20]	73.2
	[4] (Model 2)	71.4
20 < D < 35	[99]	49.8
	[112]	40.2
	[18]	44.2
40 < D < 50	[18]	48.3
	[20]	46.6
	[111]	43.3

pipe orientation the accuracy of the two phase frictional pressure drop correlations is found to decrease with increase in the pipe diameter. Table 4.16 reports the top performing correlations for three different ranges of the pipe diameter. In comparison to the horizontal and vertical upward flows, all the correlations predict the two phase frictional pressure drop data with a lower accuracy for vertical downward flow. The correlation of [18] is found to be one of the top performing correlations for all three ranges of the pipe diameter. The large inaccuracies for the pipe diameter range of 20 mm < D < 40 mm and 40 mm < D < 50 mm are probably due to the fact that most of the data for these pipe diameters belong to the annular flow regime and as mentioned earlier the two phase pressure drop correlations are found not to perform well in this flow regime. Overall, independent of the pipe orientation it is observed that the two phase pressure drop correlations do not predict the data correctly for large pipe diameters and especially in annular flow regimes.

The top performing correlations for two phase flow of nine different refrigerants in horizontal pipe orientation are shortlisted in Table 4.17. It is found that the correlations of [28, 107] are among the top performing correlations for majority of the refrigerants. The best performance is given by the correlations for R404A and R407 C with 26 and 42 data points, respectively. More data is required for these refrigerants to verify and confirm the accuracy of short listed top performing correlations. In comparison to other refrigerants, all the correlations considered in this chapter are found to give less accuracy for refrigerant R134a with 514 data points. Overall it appears that the correlations of [28, 107] have potential to predict the two phase frictional pressure drop correctly over a wide range of refrigerants and hence must be considered for any further modification to improve their accuracy. Although the correlation of [107] is not among the top performing correlations for R123, R407C, and R507 it predicts 61, 81 and 67 % of data within  $\pm 30$  % error bands. A more comprehensive analysis is required to determine the accuracies of these correlations for different flow patterns or alternatively different ranges of the void fraction for both air-water and refrigerant data.

**Table 4.17** Top performing frictional pressure drop correlations for refrigerant liquid vapor two phase flow in horizontal pipe orientation

Refrigerant	Correlation	% of data within $\pm 30$ % error bands	Standard deviation (%)
CO <sub>2</sub> (287 data points)	[28]	87	31
	[107]	85	32
	[38]	76	52
R12 (161 data points)	[28]	85	29
	[107]	78	26
	[38]	71	36
R123 (42 data points)	[28]	71	34
	[103]	74	32
	[18]	71	19
R134a (514 data points)	[28]	68	47
	[107]	67	47
	[38]	62	52
R22 (326 data points)	[18]	72	46
	[28]	75	40
	[107]	69	44
R404A (26 data points)	[64]	96	24
	[9]	88	22
	[4] (Model 2)	92	25
R407C (42 data points)	[4] (Model 1)	95	20
	[92]	93	18
	[73]	95	19
R401A (229 data points)	[28]	75	37
	[107]	68	39
	[92]	68	39
R507 (58 data points)	[18]	79	27
	[38]	74	27
	[28]	69	31

## 4.9 Application of the Recommended Void Fraction and Two Phase Frictional Pressure Drop Correlations

The objective of this section is to include some of the fundamental equations covered in this work and guide readers to select the appropriate and correct methods to solve two phase flow problems. The two problems considered here are for the air-water and refrigerant two phase flow that requires determination of void fraction and two phase pressure drop.

- (1) Consider a two component two phase flow of air-water flowing upwards in a 2.54 cm I.D. pipe 15° inclined from horizontal. The total mass flux of the mixture is 600 kg/m<sup>2</sup> s at system pressure of 7 bar and temperature of 25 °C. It is assumed that the mass flow quality of the two phase mixture remains constant at 0.095 throughout the pipe length. Calculate (a) void fraction (b) slip ratio and (c) the two phase mixture density. Verify if the use of homogeneous model approach to calculate the two phase mixture density is appropriate for this two phase flow situation.

**Solution:** For the system pressure of 7 bar and 25 °C, the physical properties of air and water are as follows.

$$\rho_l = 997.3(\text{kg/m}^3), \rho_g = 8.196(\text{kg/m}^3), \sigma = 0.0719(\text{N/m})$$

The mass flux of each liquid (water) and gas (air) phase is calculated as follows,

$$G_l = G(1 - x) = 600(\text{kg/m}^2\text{s}) \times (1 - 0.095) = 543(\text{kg/m}^2\text{s})$$

$$G_g = Gx = 600(\text{kg/m}^2\text{s}) \times 0.095 = 57(\text{kg/m}^2\text{s})$$

From the liquid and gas mass flux, the superficial velocity for each phase is calculated as,

$$U_{sl} = \frac{G_l}{\rho_l} = \frac{543(\text{kg/m}^2\text{s})}{997.3(\text{kg/m}^3)} = 0.544(\text{m/s}), U_{sg} = \frac{G_g}{\rho_{gl}} = \frac{57(\text{kg/m}^2\text{s})}{8.196(\text{kg/m}^3)} = 6.95(\text{m/s}) \text{ and}$$

$$U_m = U_{sl} + U_{sg} = 0.544(\text{m/s}) + 6.95(\text{m/s}) = 7.494(\text{m/s})$$

- (a) The selection of the appropriate void fraction correlation is based on the criteria of gas volumetric fraction ( $\beta$ ) and void fraction ( $\alpha$ ) as recommended in Table 4.10.

$$\text{The gas volumetric flow fraction is } \beta = \frac{U_{sg}}{U_{sl} + U_{sg}} = \frac{6.95}{6.95 + 0.544} = 0.927$$

From Table 4.10, for 15° upward inclined pipe orientation and  $\beta = 0.927$ , correlations of [12, 105] are recommended for two different ranges of void fraction. However, as mentioned earlier, in case of  $\beta$  shared by two different ranges of void fraction, it is recommended to calculate the void fraction using both correlations and if the void fraction predicted by Woldesemayat and Ghajar [105] is greater than 0.75 then use the larger of two values for calculation purposes. Let  $\alpha_1$  and  $\alpha_2$  be the void fractions predicted by the [12, 105] correlations, respectively. Then the final value of void fraction to be considered for the calculation purposes is the maximum of two values i.e.,  $\alpha = \max(\alpha_1, \alpha_2)$ .

Since the correlation of [12] is implicit in nature (see Table 4.2), the void fraction is calculated on an iterative basis.

The iterative calculation yields,  $C_o = 1.073$  and  $U_{gm} = 0.64$  (m/s)

Thus the void fraction from Eq. (4.4) is  $\alpha_1 = \frac{U_{sg}}{C_o U_m + U_{gm}} = \frac{6.95}{(1.073 \times 7.49) + 0.64} = 0.799$ .

Whereas, the calculation of void fraction using the correlation of [105] given in Table 4.2 is as follows,

$$C_o = \frac{U_{sg}}{U_m} \left( 1 + \left( \frac{U_{sl}}{U_{sg}} \right)^{b_1} \right) = \frac{6.95}{7.49} \left( 1 + \left( \frac{0.544}{6.95} \right)^{0.618} \right) \text{ where } b_1 = \left( \frac{\rho_g}{\rho_l} \right)^{0.1} = \left( \frac{8.196}{997.3} \right)^{0.1} = 0.618$$

$$C_o = 1.119$$

$$U_{gm} = 2.9 [g D \sigma (1 + \cos \theta) \Delta \rho / \rho_l^2]^{0.25} (1.22 + 1.22 \sin \theta)^{b_2} \text{ where } b_2 = \frac{P_{atm}}{P_{sys}} = \frac{1.013}{7} = 0.1447$$

$$U_{gm} = 2.9 \text{m}^{-0.25} \left( 9.81 (\text{m/s}^2) 0.0254 (\text{m}) \times 0.0719 (\text{N/m}) \times (1 + \cos(15)) \times \frac{(997.3 - 8.196)}{(997.3)^2} \right)^{0.25} \\ \times (1.22 + 1.22 \sin(15))^{0.1447}$$

$$U_{gm} = 0.237 (\text{m/s})$$

Thus the void fraction is calculated using Eq. (4.4),

$$\alpha_2 = \frac{U_{sg}}{C_o U_m + U_{gm}} = \frac{6.95}{(1.119 \times 7.49) + 0.237} = 0.806$$

The predictions of [12, 105] are in very good agreement with the predictions of other two top performing correlators for  $\alpha > 0.75$  and  $\beta > 0.9$ . The other two top performing correlation for this range from Table 4.7 are that of [25, 91] that predict void fraction of 0.81 and 0.779, respectively. Thus as mentioned earlier, since  $\beta$  is shared by two different ranges of void fraction and since the predicted value of void fraction is greater than 0.75, we will select the larger of the two values.

Thus the void fraction for given two phase flow condition is,  $\alpha = \alpha_2 = 0.806$ .

(b) The slip ratio is the ratio of the actual velocity of the gas phase to the actual velocity of liquid phase expressed by Eq. (4.2),

$$S = \frac{U_g}{U_l} = \frac{(U_{sg}/\alpha)}{(U_{sl}/(1-\alpha))} = \frac{(6.95/0.806)}{(0.544/(1-0.806))} = \frac{8.62}{2.804} = 3.07$$

(c) The two phase mixture density is calculated using Eq. (4.7) as follows,

$$\rho_{tp} = \rho_l (1 - \alpha) + \rho_g \alpha = 997.3 (\text{kg/m}^3) \times (1 - 0.806) + 8.196 (\text{kg/m}^3) \times (0.806) \\ = 200.1 (\text{kg/m}^3)$$

Another approach to calculate two phase mixture density is using Eq. (4.8) i.e., assuming homogeneous two phase flow (no slip between the two phases) as shown below.

$$\rho_{tp} = \left( \frac{x}{\rho_g} + \frac{1-x}{\rho_l} \right)^{-1} = \left( \frac{0.095}{8.196} + \frac{1-0.095}{997.3} \right)^{-1} = 80.01 (\text{kg/m}^3)$$

It is clear that the two phase mixture density calculated using homogeneous flow model approach is about one third of the actual density calculated using void fraction. It is shown earlier and illustrated in Fig. 4.14 that the use of homogeneous flow model to calculate two phase mixture density is appropriate when the slip ratio is close to unity. However, in this two phase flow situation, the slip ratio is 3 and hence the use of homogeneous flow model i.e., Eq. (4.8) to calculate the two phase mixture density is inappropriate.

- (2) Consider a boiling two phase flow of R134a through a 6 mm I.D. horizontal copper tube at a mass flux of  $800 \text{ kg/m}^2 \text{ s}$  and a system pressure of 1500 kPa. The two phase refrigerant enters the 1 m long tube at  $x = 0.3$  and exits at  $x = 0.7$  and assume that the quality changes linearly with the pipe length. For simplicity calculate the phase velocities, average void fraction and the frictional pressure drop at a mean quality of 0.5. Using the appropriate correlations of void fraction and frictional pressure drop, calculate (a) the average value of void fraction, two phase mixture density and hydrostatic pressure drop (b) accelerational pressure drop across the pipe length accounting for the change in two phase quality at inlet and exit (c) frictional and total two phase pressure drop and (d) what are the contributions of different components of two phase pressure drop to the total two phase pressure drop?

**Solution:** For refrigerant R134a at 1500 kPa, the thermo physical properties of liquid and vapor phase are as follows,

Saturation temperature =  $55.5 \text{ }^\circ\text{C}$ , Surface tension ( $\sigma$ ) =  $0.00427 \text{ N/m}$   
 Liquid density ( $\rho_l$ ) =  $1078 \text{ (kg/m}^3\text{)}$ , Vapor density ( $\rho_g$ ) =  $76.95 \text{ (kg/m}^3\text{)}$ ,  
 Liquid viscosity ( $\mu_l$ ) =  $0.0001746 \text{ (Pa.s)}$ , Vapor viscosity ( $\mu_g$ ) =  $0.0000138 \text{ (Pa.s)}$ .

- (a) Based on the mean quality of  $x = 0.5$  and the total mass flux of  $800 \text{ kg/m}^2\text{s}$ , the liquid and vapor phase superficial velocities are calculated as follows,

$$U_{sl} = \frac{G(1-x)}{\rho_l} = \frac{800(\text{kg/m}^2\text{s}) \times (1-0.5)}{1078(\text{kg/m}^3)} = 0.371(\text{m/s})$$

$$U_{sg} = \frac{Gx}{\rho_g} = \frac{800(\text{kg/m}^2\text{s}) \times 0.5}{76.95(\text{kg/m}^3)} = 5.198(\text{m/s}) \text{ and } U_m = U_{sl} + U_{sg} = 5.57(\text{m/s})$$

As recommend in Table 4.10, for horizontal two phase flow of refrigerants, the correlation of [105] can be used for the entire range of void fraction and gas volumetric flow fraction.

The distribution parameter and drift velocity required in this correlation as given in Table 4.2 is calculated as shown below,

$$C_o = \frac{U_{sg}}{U_m} \left( 1 + \left( \frac{U_{sl}}{U_{sg}} \right)^{b_1} \right) = \frac{5.198}{5.57} \left( 1 + \left( \frac{0.371}{5.198} \right)^{0.768} \right) \text{ where } b_1 = \left( \frac{\rho_g}{\rho_l} \right)^{0.1} = \left( \frac{76.95}{1078} \right)^{0.1} = 0.768$$

$$C_o = 1.056$$

$$U_{gm} = 2.9 [gD\sigma(1 + \cos \theta)\Delta\rho/\rho_l^{2.7}]^{0.25} (1.22 + 1.22 \sin \theta)^{b_2} \text{ where } b_2 = \frac{P_{am}}{P_{sys}} = \frac{101.32(kPa)}{1500(kPa)} = 0.0675$$

$$U_{gm} = 2.9m^{-0.25} \left( 9.81(m/s^2)0.006(m) \times 0.00427(N/m) \times (1 + \cos(0)) \times \frac{(1078 - 76.95)}{(1078)^2} \right)^{0.25} \\ \times (1.22 + 1.22 \sin(0))^{0.0675}$$

$$U_{gm} = 0.0754(m/s)$$

Thus the void fraction is calculated using Eq. (4.4) as shown below,

$$\alpha = \frac{U_{sg}}{C_o U_m + U_{gm}} = \frac{5.198}{(1.056 \times 5.57) + 0.0754} = 0.872$$

Based on the void fraction, the two phase mixture density is calculated using Eq. (4.7).

$$\rho_{tp} = \rho_l(1 - \alpha) + \rho_g \alpha = 1078(\text{kg/m}^3) \times (1 - 0.872) + 76.95(\text{kg/m}^3) \times (0.872) \\ = 205.1(\text{kg/m}^3)$$

For horizontal pipe orientation, the hydrostatic pressure drop is zero. i.e.,  $\left(\frac{dP}{dL}\right)_h = 0$ . Otherwise for any other orientation it is calculated using Eq. (4.6).

(b) Given that the flow quality changes from 0.3 to 0.7 from pipe inlet to exit, the acceleration component of two phase pressure drop is calculated using Eq. (4.9).

$$\left(\frac{dP}{dL}\right)_a = \frac{1}{L} \left\{ \left[ \frac{G_l^2}{\rho_l(1 - \alpha)} + \frac{G_g^2}{\rho_g \alpha} \right]_{out} - \left[ \frac{G_l^2}{\rho_l(1 - \alpha)} + \frac{G_g^2}{\rho_g \alpha} \right]_{in} \right\}$$

For the inlet and exit quality of 0.3 and 0.7, the liquid and vapor mass flux are calculated as follows,

At pipe inlet for  $x = 0.3$ ,

$$G_l = G(1 - x) = 800(\text{kg/m}^2\text{s}) \times (1 - 0.3) = 560(\text{kg/m}^2\text{s}),$$

$$G_g = Gx = 800(\text{kg/m}^2\text{s}) \times 0.3 = 240(\text{kg/m}^2\text{s})$$

Similarly at the pipe outlet for  $x = 0.7$ ,

$$G_l = G(1 - x) = 800(\text{kg/m}^2\text{s}) \times (1 - 0.7) = 240(\text{kg/m}^2\text{s}),$$

$$G_g = Gx = 800(\text{kg/m}^2\text{s}) \times 0.7 = 560(\text{kg/m}^2\text{s})$$

Based on the inlet and outlet mass flux, the superficial velocity of each phase is calculated as

At pipe inlet,

$$U_{sl} = \frac{G_l}{\rho_l} = \frac{560(\text{kg/m}^2\text{s})}{1078(\text{kg/m}^3)} = 0.519(\text{m/s}),$$

$$U_{sg} = \frac{G_g}{\rho_g} = \frac{240(\text{kg/m}^2\text{s})}{76.95(\text{kg/m}^3)} = 3.118(\text{m/s}), U_m = 3.637(\text{m/s})$$

At pipe outlet,

$$U_{sl} = \frac{G_l}{\rho_l} = \frac{240(\text{kg/m}^2\text{s})}{1078(\text{kg/m}^3)} = 0.223(\text{m/s}),$$

$$U_{sg} = \frac{G_g}{\rho_g} = \frac{560(\text{kg/m}^2\text{s})}{76.95(\text{kg/m}^3)} = 7.277(\text{m/s}), U_m = 7.5(\text{m/s})$$

Based on the phase superficial velocities, the distribution parameter using [105] at pipe inlet and outlet are found to be  $C_o = 1.073$  and  $C_o = 1.037$ , respectively. The drift velocity of [105] correlation is independent of the phase velocities and hence remains unchanged i.e.,  $U_{gm} = 0.0754$  (m/s) at pipe inlet and outlet.

The void fraction based on the phase velocities and distribution parameter calculated above gives,  $\alpha_{in} = 0.783$  and  $\alpha_{out} = 0.926$ .

The acceleration pressure drop is,

$$\left(\frac{dP}{dL}\right)_a = \left\{ \left[ \frac{240^2}{1078(1-0.926)} + \frac{560^2}{76.95 \times 0.926} \right]_{out} - \left[ \frac{560^2}{1078(1-0.783)} + \frac{240^2}{76.95 \times 0.783} \right]_{in} \right\} = 2826.5 \left(\frac{\text{Pa}}{\text{m}}\right)$$

- (c) From Table 4.17, the recommended correlations for two phase flow of R134a in a horizontal pipe are those of [28, 38, 107]. The [28] correlation is based on the concept of homogeneous flow model while the correlations of [38, 107] are based on the separated flow model concept. We will use the correlation of [107] for this problem.

From Table 4.12, the two phase frictional multiplier for [107] is determined from the following equation,

$$\Phi_{lo}^2 = \left\{ Y^2 x^3 + (1-x)^{0.33} (1 + 2x(Y^2 - 1)) \right\} \left[ 1 + 1.54(1-x)^{0.5} La \right]$$

$$\text{where, } Y = \sqrt{\frac{(dP/dL)_{go}}{(dP/dL)_{lo}}} \text{ and } La = \sqrt{\left( \frac{\sigma}{g(\rho_l - \rho_g)} \right) / D}$$

It should be noted that the [107] recommend use of [34] correlation for determination of single phase friction factor  $f_{go}$  and  $f_{lo}$ .

The [34] correlation for single phase turbulent flow is given as,

$$f_{lo} = 0.25 \left( \log \left( \frac{150.39}{\text{Re}_{lo}^{0.98865}} - \frac{152.66}{\text{Re}_{lo}} \right) \right)^{-2} \text{ and } f_{go} = 0.25 \left( \log \left( \frac{150.39}{\text{Re}_{go}^{0.98865}} - \frac{152.66}{\text{Re}_{go}} \right) \right)^{-2}$$

The Reynolds number required in the above equation is defined for liquid and gas phases as shown in following equations,

$$\text{Re}_{lo} = \frac{GD}{\mu_l} = \frac{800(\text{kg/m}^2\text{s}) \times 0.006(\text{m})}{0.0001746} = 27491 \text{ and}$$

$$\text{Re}_{go} = \frac{GD}{\mu_g} = \frac{800(\text{kg/m}^2\text{s}) \times 0.006(\text{m})}{0.0000138} = 347826$$

Thus from the friction factor equation of [34] we get,

$$f_{lo} = 0.02398 \text{ and } f_{go} = 0.01407.$$

The single phase pressure drop for liquid and gas phases are calculated from Eqs. (4.16) and (4.17),

$$\left( \frac{dP}{dL} \right)_{lo} = \frac{f_{lo} G^2}{2D\rho_l} = \frac{0.02398 \times 800^2(\text{kg/m}^2\text{s})^2}{2 \times 0.006(\text{m}) \times 1078(\text{kg/m}^3)} = 1186 \left( \frac{\text{Pa}}{\text{m}} \right) \text{ and}$$

$$\left( \frac{dP}{dL} \right)_{go} = \frac{f_{go} G^2}{2D\rho_g} = \frac{0.01407 \times 800^2(\text{kg/m}^2\text{s})^2}{2 \times 0.006(\text{m}) \times 76.95(\text{kg/m}^3)} = 9752 \left( \frac{\text{Pa}}{\text{m}} \right)$$

Thus,  $Y = \sqrt{\frac{9752(\text{Pa/m})}{1186(\text{Pa/m})}} = 2.867$  and the Laplace number is calculated to be,  $\text{La} = 0.1099$ .

Thus the two phase frictional multiplier is found to be,

$$\Phi_{lo}^2 = \left\{ 2.867^2 \times 0.5^3 + (1 - 0.5)^{0.33} (1 + 2 \times 0.5(2.867^2 - 1)) \right\} [1 + 1.54(1 - 0.5)^{0.5} 0.1099] = 8.455$$

Now, the two phase frictional pressure drop is determined using Eq. (4.16) as,

$$\left( \frac{dP}{dL} \right)_{w,f} = \Phi_{lo}^2 \left( \frac{dP}{dL} \right)_{lo} = 8.455 \times 1186 \left( \frac{\text{Pa}}{\text{m}} \right) = 10028 \left( \frac{\text{Pa}}{\text{m}} \right)$$

The total two phase pressure drop is the sum of hydrostatic, accelerational and frictional two phase pressure drops expressed by Eq. (4.5) as,

$$\left( \frac{dP}{dL} \right)_{t,tp} = \left( \frac{dP}{dL} \right)_h + \left( \frac{dP}{dL} \right)_f + \left( \frac{dP}{dL} \right)_a = 0 + 10028 + 2826.5 = 12854.5 \left( \frac{\text{Pa}}{\text{m}} \right)$$

- (c) It is found that the accelerational pressure drop contributes to about 22 % of the total two phase pressure drop while the remaining 78 % contribution is due to the frictional two phase pressure drop. It should be noted that in case of adiabatic two phase flow, the quality and void fraction at pipe inlet and exit remain practically unchanged and hence the accelerational two phase pressure drop may be neglected.

## 4.10 Concluding Remarks

The purpose of this work is fulfilled by a brief and insightful discussion about the two phase flow patterns, void fraction and pressure drop. The two phase flow patterns are elucidated with the help of still photographs and their transition from one flow pattern to another is explained with the help of flow pattern maps. The void fraction and two phase pressure drop data used for both air-water and refrigerants are one of the most comprehensive data ever used for the performance assessment of void fraction and two phase pressure drop correlations. This data bank has been of great help not only for the performance assessment of the correlations but has also contributed to better understanding of the two phase flow phenomenon through a parametric analysis of the two phase void fraction and pressure drop with respect to the variables such as, flow patterns, pipe diameter and pipe orientation.

A comprehensive scrutiny of the void fraction and two phase pressure drop correlations for several two phase flow conditions has resulted in recommendations of the top performing correlations for different cases. Based on the recommendations of Table 4.10, only two correlations of [12, 105], can be used to predict the void fraction with fair accuracy in both one component and two component two phase flow over a range of pipe diameters and pipe orientations. However, more experimental data is required in the low region of void fraction typically  $\alpha < 0.5$  in both upward and downward inclined pipe orientations to validate and further improve their performance in these orientations. It is observed that, the correlation of [107] has good potential to predict the two phase frictional pressure drop and may be considered for further analysis and modification to account for the two phase flow of different refrigerants. This work is concluded by providing two sample problems that deal with air-water and refrigerant two phase flow under different operating conditions. The objective of this exercise is achieved by explaining the selection process of the recommended correlations for void fraction and two phase pressure drop in addition to highlighting some of the fundamental concepts.

**Acknowledgements** The authors are thankful to Dr. John Thome (EPFL, Switzerland), Dr. Josua Meyer (University of Pretoria, South Africa), Dr. Somchai Wongwises (KMUTT, Thailand) and Dr. Neima Brauner (Tel Aviv University, Israel) for sharing void fraction and pressure drop data.

## References

1. W.W. Akers, A. Deans, O.K. Crosslee, Condensing heat transfer within horizontal tubes. *Chem. Eng. Prog.* **55**, 171–176 (1959)
2. S. Al-lababidi, A. Addali, H. Yeung, D. Mba, F. Khan, Gas void fraction measurement in two phase gas liquid slug flow using acoustic emission technology. *Trans. ASME* **131**, 501–507 (2009)
3. P. Alia, L. Cravarolo, A. Hassid, E. Pedrocchi, Liquid volume fraction in adiabatic two-phase vertical upflow in round conduits C.I.S.E, 1965
4. M.M. Awad, Y.S. Muzychka, Effective property models for homogeneous two-phase flows. *Exp. Thermal Fluid Sci.* **33**, 106–113 (2008)
5. S. Badie, C.P. Hale, G.F. Hewitt, Pressure gradient and holdup in horizontal two phase gas-liquid flows with low liquid loading. *Int. J. Multiph. Flow* **26**, 1525–1543 (2000)
6. S.G. Bankoff, A variable density single fluid model for two phase flow with particular reference to steam-water flow. *J. Heat Transfer* **11**, 165–172 (1960)
7. C.J. Barcozy, A systematic correlation for two phase pressure drop. *Chem. Eng. Prog.* **62**(44), 232–249 (1966)
8. D.R.H. Beattie, S. Sugawara, Steam-water void fraction for vertical upflow in a 73.9 mm pipe. *Int. J. Multiph. Flow* **12**(4), 641–653 (1986)
9. D.R.H. Beattie, P.B. Whalley, A simple two-phase frictional pressure drop calculation method. *Int. J. Multiphase Flow: Brief Commun.* **8**(1), 83–87 (1982)
10. H.D. Beggs, An experimental study of two phase flow in inclined pipes. Ph.D. thesis, University of Tulsa, 1972
11. D. Bestion, The physical closure laws in the CATHARE code. *Nucl. Eng. Des.* **124**, 229–245 (1990)
12. S.M. Bhagwat, A.J. Ghajar, Flow patterns and pipe orientation independent semi-empirical void fraction correlation for a gas-liquid two-phase flow based on the concept of drift flux model. Paper presented at the ASME 2012 Summer Heat Transfer Conference, Puerto Rico, 2012
13. S.M. Bhagwat, A.J. Ghajar, Similarities and differences in the flow patterns and void fraction in vertical upward and downward two phase flow. *Exp. Thermal Fluid Sci.* **39**, 213–227 (2012). doi:[10.1016/j.expthermflusci.2012.01.026](https://doi.org/10.1016/j.expthermflusci.2012.01.026)
14. H. Blasius, Das Anhlichkeitsgesetz bei Reibungsvorgangen in Flussigkeiten Gebiete *Ingenieurw* 131, 1913
15. R.H. Bonnecaze, Greskovich E.J. Erskine, Holdup and Pressure Drop for Two Phase Slug Flow in Inclined Pipelines. *AIChE* **17**, 1109–1113 (1971)
16. C.D. Bowers, P.S. Hrnjak, Determination of void fraction in separated two phase flows using optical techniques. Paper presented at the international refrigeration and air-conditioning conference paper 1083, Purdue, 2010
17. J. Cai, T. Chen, Q. Ye, Void fraction in bubbly and slug flow in downward air-oil two phase flow in vertical tubes. Paper presented at the international symposium on multiphase flow, Beijing, 1997
18. A. Cavallini, G. Censi, D. Del Col, L. Doretti, G.A. Longo, L. Rossetto, Condensation of halogenated refrigerants inside smooth tubes. *HVAC&R Res.* **8**, 429–451 (2002)
19. J.J. Chen, A further examination of void fraction in annular two-phase flow. *Int. J. Heat Mass Transf.* **29**, 4269–4272 (1986)
20. D. Chisholm, Pressure gradients due to the friction during the flow of evaporating two phase mixtures in smooth tubes and channels. *Int. J. Heat Mass Transf.* **16**, 347–358 (1973)
21. J. Choi, E. Pereyra, C. Sarica, C. Park, J.M. Kang, An efficient drift flux closure relationship to estimate liquid holdups of gas-liquid two phase flow in pipes. *Energies* **5**, 5294–5306 (2012)
22. R. Chokshi, Prediction of pressure drop and liquid holdup in vertical two phase flow through large diameter tubing. Ph.D. thesis, University of Tulsa, 1994

23. S.W. Churchill, Friction factor equation spans all fluid- flow regimes. *Chem. Eng.* **7**, 91–92 (1977)
24. A. Ciccihitti, C. Lombardi, M. Silvestri, R. Soldaini, G. Zavatarelli, Two-phase cooling experiments: pressure drop, heat transfer and burnout measurements. *Energ. Nucl.* **7**, 407–429 (1960)
25. A. Cioncoloni, J.R. Thome, Void fraction prediction in annular two phase flow. *Int. J. Multiph. Flow* **43**, 72–84 (2012)
26. N.N. Clark, R.L. Flemmer, Predicting the Holdup in two phase bubble upflow and downflow using the Zuber and Findlay drift flux model. *AIChE* **31**(3), 500–503 (1985)
27. C.F. Colebrook, Turbulent flow in pipes, with particular reference to the transition between the smooth and rough pipe laws. *J. Inst. Civ. Eng.* **11**, 1938–1939 (1939)
28. W.F. Davidson, P.H. Hardie, C.G.R. Humphreys, A.A. Markson, A.R. Mumford, T. Ravese, Studies of heat transmission through boiler tubing at pressures from 500–3300 lbs. *Trans. ASME* **65**(6), 553–591 (1943)
29. R. De Rauz, Taux de vide et glissement dans un ecoulement biphasé ascendant et descendant CENG Note TTN 165, 1976
30. A.E. Dukler, M. Wicks, R.G. Cleveland, Frictional pressure drop in two phase flow: Part A and B. *AIChE* **10**, 38–51 (1964)
31. K.J. Elkow, Void fraction measurement and Analysis at normal gravity and microgravity conditions. M.S. thesis, University of Saskatchewan, 1995
32. M. Espedal, K. Bendiksen, Onset of instabilities and slugging in horizontal and near horizontal gas liquid flow. Paper presented at the European two phase flow group meeting, Paris, France, 1989
33. Y.Q. Fan, Q. Wang, H.Q. Zhang, C. Sarica, Experimental study of air-water and air-oil low liquid loading horizontal two phase flow in pipes, 2007
34. X.D. Fang, Y. Xu, Z.R. Zhou, New correlations of single phase friction factor for turbulent pipe flow and evaluation of existing single phase friction factor correlations. *Nucl. Eng. Des.* **241**, 897–902 (2011)
35. R.C. Fernandes, Experimental and theoretical studies of isothermal upward gas-liquid flows in vertical tubes. Ph.D. thesis, University of Houston, 1981
36. M. Fourar, S. Boris, Experimental study of air water two phase flow through a fracture. *Int. J. Multiph. Flow* **4**, 621–637 (1995)
37. H. Franca, R.T. Lahey, The use of drift flux techniques for the analysis of horizontal two phase flows. *Int. J. Multiph. Flow* **18**, 787–801 (1992)
38. L. Friedel, Improved friction pressure drop correlation for horizontal and vertical two phase pipe flow. *Eur. Two Phase Flow Group Meet. Pap.* **18**, 485–492 (1979)
39. L. Friedel, Two-phase frictional pressure drop correlation for vertical downflow. *Ger. Chem. Eng.* **8**(1), 32–40 (1985)
40. F. Garcia, R. Garcia, J.C. Padrino, C. Mata, J.L. Trallero, D.D. Joseph, Power law and composite power law friction factor correlations for laminar turbulent gas liquid flow in horizontal pipe lines. *Int. J. Multiph. Flow* **29**(10), 1605–1624 (2003)
41. A.J. Ghajar, S.M. Bhagwat, Effect of void fraction and two-phase dynamic viscosity models on prediction of hydrostatic and frictional pressure drop in vertical upward gas-liquid two phase flow. *Heat Transfer Eng.* **34**(13), 1044–1059 (2013)
42. A.J. Ghajar, C.C. Tang, Advances in void fraction, flow pattern maps and non-boiling heat transfer two phase flow in pipes with various inclinations. *Adv. Multiph. Flow Heat Transfer* **1**, 1–52 (2009) (Chapter 1)
43. A.J. Ghajar, C.C. Tang, Void fraction and flow patterns of two phase flow in upward, downward vertical and horizontal pipes. *Adv. Multiph. Flow Heat Transfer* **4**, 175–201 (2012) (Chapter 7)
44. H. Goda, T. Hibiki, S. Kim, M. Ishii, J. Uhle, Drift flux model for downward two phase flow. *Int. J. Heat Mass Transf.* **46**, 4835–4844 (2003)

45. L.E. Gomez, O. Shoham, Z. Schmidt, R.N. Choshki, T. Northug, Unified mechanistic model for steady state two phase flow: horizontal to upward vertical flow. *Soc. Petrol. Eng.* **5**, 339–350 (2000)
46. D.M. Graham, T.A. Newell, J.C. Chato, Experimental investigation of void fraction during refrigerant condensation. University of Illinois, Urbana Champaign, 1997
47. E.J. Greskovich, W.T. Cooper, Correlation and prediction of gas-liquid holdups in inclined upflows. *AIChE* **21**, 1189–1192 (1975)
48. R. Gronnerud, Investigation of liquid holdup, flow resistance and heat transfer in circulation type of evaporators, part iv: two phase flow resistance in boiling refrigerants Annexe 1972-1, *Bull de l'Inst Froid*, 1979
49. A.R. Hasan, Void fraction in bubbly and slug flow in downward vertical and inclined systems. *Soc. Petrol. Eng. Prod. Facil.* **10**(3), 172–176 (1995)
50. A. Hernandez, Experimental research on downward two phase flow. Paper presented at the SPE annual technical conference and exhibition San Antonio, TX-U.S.A, 2002
51. G.F. Hewitt, C.J. Martin, N.S. Wilkes, Experimental and modeling studies of churn-annular flow in the region between flow reversal and the pressure drop minimum. *Physicochem. Hydrodyn.* **6**(1/2), 69–86 (1985)
52. T. Hibiki, M. Ishii, One-dimensional drift flux model and constitutive equations for relative motion between phases in various two-phase flow regimes. *Int. J. Heat Mass Transf.* **46**, 4935–4948 (2003)
53. D. Jowitt, C.A. Cooper, K.G. Pearson, The thetis 80 % blocked cluster experiments part 5: level swell experiments safety and engineering science, 1984
54. D.S. Jung, R. Radermacher, Prediction of pressure drop during horizontal annular flow boiling of pure and mixed refrigerants. *Int. J. Heat Mass Transf.* **32**(12), 2435–2446 (1989)
55. M. Kaji, B.J. Azzopardi, The effect of pipe diameter on the structure of gas-liquid flow in vertical pipes. *Int. J. Multiph. Flow* **36**(4), 303–313 (2010)
56. I. Kataoka, M. Ishii, Drift flux model for large diameter pipe and new correlation for pool void fraction. *Int. J. Heat Mass Transfer* **30**, 1927–1939 (1987)
57. K. Kawanishi, Y. Hirao, A. Tsuge, An experimental study on drift flux parameters for two phase flow in vertical round tubes. *Nucl. Eng. Des.* **120**, 447–458 (1990)
58. K.D. Kerpel, B. Ameel, C. T'Joel, H. Caniere, M. De-Paepe, Flow regime based calibration of a capacitive void fraction sensor for small diameter tubes. *Int. J. Refrig.* **36**(2), 390–401 (2013)
59. S.L. Kokal, J.F. Stainslav, An experimental study of two phase flow in slightly inclined pipes II: liquid holdup and pressure drop. *Chem. Eng. Sci.* **44**, 681–693 (1989)
60. S. Koyoma, J. Lee, R. Yonemoto, An investigation on void fraction of vapor-liquid two phase flow for smooth and microfin tubes with R134a at adiabatic condition. *Int. J. Multiph. Flow* **30**, 291–310 (2004)
61. C.W. Lau, Bubbly and slug flow pressure drop in inclined pipe. BS thesis, MIT, 1972
62. T.W. Lim, Flow pattern and pressure drop of pure refrigerants and their mixtures in horizontal tube. *J. Mech. Sci. Technol.* **19**(12), 2289–2295 (2005)
63. T.W. Lim, Y. Fujita, Flow pattern and pressure drop in flow boiling of pure refrigerants and their mixture in horizontal tube. *Mem. Fac. Eng., Kyushu Univ.* **62**(1), 41–54 (2002)
64. S. Lin, C.C.K. Kwok, R.Y. Li, Z.H. Chen, Z.Y. Chen, Local frictional pressure drop during vaporization of R12 through capillary tubes. *Int. J. Multiph. Flow* **17**, 95–102 (1991)
65. S. Lips, J.P. Meyer, Experimental study of convective condensation in an inclined smooth tube. part II: inclination effect on pressure drop and void fraction. *Int. J. Heat Mass Transf.* **55**, 405–412 (2012)
66. R.W. Lockhart, R.C. Martinelli, Proposed correlation of data for isothermal two phase, two component flow in pipes. *Chem. Eng. Prog.* **45**, 39–48 (1949)
67. A. Lorenzi, G. Stogia, Downward two phase flow: experimental investigation. *Energia Nucleare* **23**(7), 396–401 (1976)
68. Z.S. Mao, A.E. Dukler, The myth of churn flow. *Int. J. Multiph. Flow* **19**(2), 377–383 (1993)

69. R.C. Martinelli, D.B. Nelson, Prediction of pressure drop during forced circulation boiling of water. *Trans. ASME* **90**, 695–702 (1948)
70. L. Mattar, G.A. Gregory, Air-oil slug flow in upward inclined pipe—I slug velocity, holdup and pressure gradient. *J. Can. Pet. Technol.* **13**, 69–76 (1974)
71. W.H. McAdams, W.K. Woods, L.V. Heroman, Vaporization inside horizontal tubes—II benzene oil mixtures. *Trans. ASME* **64**, 193–200 (1942)
72. K. Minami, J.P. Brill, Liquid holdup in wet gas pipelines. *Soc. Petrol. Eng.* **2**, 36–44 (1987)
73. K. Mishima, T. Hibiki, Some characteristics of air-water two phase flow in small diameter vertical tubes. *Int. J. Multiph. Flow* **22**(4), 703–712 (1996)
74. H. Mukherjee, An experimental study of inclined two phase flow. Ph.D. thesis, The University of Tulsa, 1979
75. H. Muller-Steinhagen, K. Heck, A simple friction pressure drop correlation for two-phase flow in pipes. *Chem. Eng. Process* **20**, 297–308 (1986)
76. V.T. Nguyen, Two phase gas-liquid cocurrent flow : an investigation of holdup, pressure drop and flow patterns in a pipe at various inclinations. Ph.D. thesis, The University of Auckland, 1975
77. C.R. Nichols, A study of vertical flow of air-water mixture. Ph.D. thesis, University of Maryland, 1965
78. R. Oliemans, Two phase flow in gas transmission pipelines. Paper presented at the Petroleum Division ASME Meeting, Mexico, 1976
79. N.K. Omebere-Iyari, B.J. Azzopardi, A study of flow patterns for gas-liquid flow in small diameter tubes. *Chem. Eng. Res. Des.* **85**(A2), 180–192 (2007)
80. O. Oshinowo, Two phase flow in a vertical tube coil. Ph.D. thesis, University of Toronto, 1971
81. M. Ottens, H.C.J. Hoefsloot, P.J. Kamersma, Correlations predicting liquid holdup and pressure gradient in steady state nearly horizontal cocurrent gas-liquid pipe flow. *Inst. Chem. Eng. Trans. IChemE* **79** (A), 581–592 (2001)
82. G. Paras, Characterization of downward two phase flow by neutron noise analysis. MS thesis, University of Washington, 1982
83. A. Permoli, D. Francesco, A. Prima, An empirical correlation for evaluating two phase mixture density under adiabatic conditions. Paper presented at the European two phase flow group meeting Milan, Italy, 1970
84. J.M. Quiben, J.R. Thome, Flow pattern based two phase frictional pressure drop model for horizontal tubes. Part II: new phenomenological model. *Int. J. Heat Fluid Flow* **28**, 1060–1072 (2007)
85. R. Revellin, J.R. Thome, Adiabatic two phase frictional pressure drop in microchannels. *Exp. Thermal Fluid Sci.* **31**, 673–685 (2007)
86. S.Z. Rouhani, E. Axelsson, Calculation of void volume fraction in the subcooled and quality boiling regions. *Int. J. Heat Mass Transf.* **13**, 383–393 (1970)
87. P.S. Sacks, Measured characteristics of adiabatic and condensing single component two phase flow of refrigerant in a 0.377 inch diameter horizontal tube. Paper presented at the ASME winter annual meeting, Houston, Texas, 1975
88. K. Sekoguchi, Y. Saito, T. Honda, JSME Reprint No. 700. 7:83, 1970
89. T.A. Shedd, Void fraction and pressure drop measurements for refrigerant R410a flows in small diameter tubes, 2010
90. D.G. Shipley, Two phase flow in large diameter pipes. *Chem. Eng. Sci.* **39**, 163–165 (1982)
91. S.L. Smith, Void fraction in two phase flow: a correlation based on an equal velocity head model. *Inst. Mech. Eng.* **184**(Part 1), 647–657 (1969)
92. A.L. Souza, M.M. Pimenta, Prediction of pressure drop during horizontal two phase flow of pure and mixed refrigerants. Paper presented at the ASME conference on cavitation and multiphase flow, HTD, 1995
93. P.L. Spedding, J.J. Chen, Holdup in two phase flow. *Int. J. Multiph. Flow* **10**, 307–339 (1984)

94. M. Sujumng, Heat transfer, pressure drop and void fraction in two phase two component flow in vertical tube. Ph.D. thesis, The University of Manitoba, 1997
95. K.H. Sun, R.B. Duffey, C.M. Peng, The prediction of two phase mixture level and hydrodynamically controlled dryout under low flow conditions. *Int. J. Multiph. Flow* **7**, 521–543 (1981)
96. L. Sun, K. Mishima, Evaluation analysis of prediction methods for two phase flow pressure drop in mini channels. *Int. J. Multiph. Flow* **35**, 47–54 (2009)
97. K. Takeuchi, M.Y. Young, L.E. Hochreiter, Generalized drift flux correlation for vertical flow. *Nucl. Sci. Eng.* **112**, 170–180 (1992)
98. J.R.S. Thom, Prediction of pressure drop during forced circulation boiling of water. *Int. J. Heat Mass Transf.* **7**(7), 709–724 (1964)
99. T.N. Tran, Y.C. Chu, M.W. Wambsganss, D.M. France, Two phase pressure drop of refrigerants during flow boiling in small channels: an experimental investigation and correlation development. *Int. J. Multiph. Flow* **26**, 1739–1754 (2000)
100. X. Tu, P.S. Hrnjak, Pressure drop characteristics of R134a two phase flow in a horizontal rectangular microchannel. Paper presented at the international mechanical engineering congress and exposition, New Orleans, USA, 2002
101. J.M. Turner, G.B. Wallis, The separate cylinders model of two phase flow Thayer's School of Engineering, Dartmouth College, 1965
102. K. Usui, K. Sato, Vertically downward two phase flow (I) void distribution and average void fraction. *J. Nucl. Sci. Technol.* **26**(7), 670–680 (1989)
103. C.C. Wang, S.K. Chiang, Y.J. Chang, T.W. Chung, Two phase flow resistance of refrigerants R22, R410A and R407C in small diameter tubes. *Inst. Chem. Eng., Trans. IChemE* **79**, 553–560 (2001)
104. L. Wojtan, T. Ursenbacher, J.R. Thome, Measurement of dynamic void fractions in stratified types of flow. *Exp. Thermal Fluid Sci.* **29**, 383–392 (2005)
105. M.A. Woldesemayat, A.J. Ghajar, Comparison of void fraction correlations for different flow patterns in horizontal and upward inclined pipes. *Int. J. Multiph. Flow* **33**, 347–370 (2007)
106. S. Wongwises, M. Pipathtakul, Flow pattern, pressure drop and void fraction of gas-liquid two phase flow in an inclined narrow annular channel. *Exp. Thermal Fluid Sci.* **30**, 345–354 (2006)
107. Y. Xu, X. Fang, A new correlation of two phase frictional pressure drop for evaporating two phase flow in pipes. *Int. J. Refrig.* **35**, 2039–2050 (2012)
108. Y. Xu, X. Fang, X. SU, Z. Zhou, W. Chen, Evaluation of frictional pressure drop correlations for two-phase flow in pipes. *Nucl. Eng. Des.* **253**, 86–97 (2012)
109. D.A. Yashar, T.A. Newell, J.C. Chato, Experimental investigation of void fraction during horizontal flow in smaller diameter refrigeration applications. ACRC TR-141 University of Illinois, Urbana Champaign, 1998
110. J. Yijun, K. Rezkallah, A study on void fraction in vertical co-current upward and downward two-phase gas-liquid flow—I: experimental results. *Chem. Eng. Commun.* **126**, 221–243 (1993)
111. S.H. Yoon, E.S. Cho, Y.W. Hwang, M.S. Kim, K. Min, Y. Kim, Characteristics of evaporative heat transfer and pressure drop of carbon dioxide and correlation development. *Int. J. Refrig.* **27**, 111–119 (2004)
112. W. Zhang, T. Hibiki, K. Mishima, Correlations of two phase frictional pressure drop and void fraction in mini-channel. *Heat Mass Transf.* **53**, 433–465 (2010)
113. H.D. Zhao, K.C. Lee, D.H. Freeston, Geothermal two phase flow in horizontal pipes. Paper presented at the proceedings of world geothermal congress, Tokyo, Japan, 2000
114. S.M. Zivi, Estimation of steady state steam void fraction by means of the principle of minimum entropy production. *Trans. ASME, J. Heat Transfer* **86**, 247–252 (1964)